**Instrument Science Report HST+COS 2018**

# Cycle 21-24 HST+COS Target Acquisition Monitoring

Steven V. Penton

April 9, 2018

ABSTRACT

*This ISR documents the Cosmic Origins Spectrograph (COS) Target Acquisition (TA) monitoring programs for HST Cycles 21–24. During this period, FUV exposures were executed at Lifetime Positions LP2 and LP3, and all NUV exposures were obtained at the nominal (LP1) position. These programs were designed to monitor numerous aspects of both imaging and spectroscopic COS TAs, including checking the TA subarrays, monitoring the required flashes of the internal PtNe lamps, and evaluating the accuracy of numerous COS flight software (FSW) patchable constants required for TA. This project verified that all three COS TA modes (FUV spectroscopic, NUV spectroscopic, and NUV imaging) were, on large, behaving nominally in Cycle 21-24, and determined that no SIAF or FSW parameter updates were required during this time, with the exception of changes to MIRRORB* `ACQ/IMAGE` *MIRRORB in 2014. These changes included a changing of the lamp current from LOW to MEDIUM, an adjustment of the* `LTACAL` *exposure time, and a modification of both the MIRRORB WCA and PSA/BOA* `ACQ/IMAGE` *TA subarrays.*

# Contents

# List of Figures

# List of Tables

# 1 Introduction

Preliminary results of the Hubble Space Telescopes' (HST) Cosmic Origins Spectrograph (COS) target acquisition (TA) programs reviewed here were previously reported in the following COS ISRs:

- COS ISR 2015-02 (Summary of the COS Cycle 20 Calibration Program)
- COS ISR 2015-06 (Summary of the COS Cycle 21 Calibration Program)
- COS ISR 2016-03 (Summary of the COS Cycle 22 Calibration Program)
- COS ISR 2016-09 (Cycle 22 COS Target Acquisition Monitor Summary)
- COS ISR 2017-18 (Cycle 23 COS Target Acquisition Monitor Summary)
- COS ISR 2018-09 (Cycle 24 COS Target Acquisition Monitor Summary)

The information in this ISR supercedes any previous preliminary results or conclusions.

This ISR provides the full details of the following HST+COS calibration **P**rograms:

- **P**13124 (COS Imaging TA and Spectroscopic WCA-PSA/BOA offset verifications, Cycle 20)
- **P**13526 (COS Imaging TA and Spectroscopic WCA-PSA/BOA offset verifications, Cycle 21)
- **P**13972 (COS Imaging TA and Spectroscopic WCA-PSA/BOA offset verifications, Cycle 22)
- **P**14440 (COS Imaging TA and Spectroscopic WCA-PSA/BOA offset verifications, Cycle 23)
- **P**14857 (COS Imaging TA and Spectroscopic WCA-PSA/BOA offset verifications, Cycle 24)

## 1.1 Introductory Notes and Conventions

There are a few COS conventions to be established before discussing the TA monitoring in detail.

1. COS TAs are performed in raw or "detector" coordinates, not the "user" coordinate system of calibrated COS files. To avoid confusion over the different coordinate systems, we will use along-dispersion (AD) and cross-dispersion (XD) whenever possible. All references to the coordinates "X" and "Y" are in the detector coordinate system unless otherwise specified. In raw NUV coordinates, +X is -XD and +Y is -AD. In raw FUV coordinates, +X is -AD and +Y is +XD. The transformations between user and detector coordinates are :

$$NUV : X_{user} = 1023 - Y_{detector} \tag{1}$$

$$NUV : Y_{user} = 1023 - X_{detector} \tag{2}$$

$$FUV : X_{user} = 16383 - X_{detector} \tag{3}$$

$$FUV : Y_{user} = Y_{detector} \tag{4}$$

2. When referencing NUV pixels, we will abbreviate pixel as p. For the FUV, we use DE (or rows/columens) to reference the FUV digital elements.

3. When discussing the various subarrays used during COS TA, boxes will be specified by giving the lowest valued corner (C) and full size (S) for both X and Y. A box is fully specified by giving its XC, XS, YC, & YS. In this TIR, these will always be given in detector coordinates.

4. To clarify the names and locations of various TA parameters, the following convention will be used :
   - COS TA modes and their optional parameters will be in `Courier` (e.g., `ACQ/IMAGE` and `NUM_POS`).
   - Keywords in FITS headers will be in *ITALICIZED ALL CAPITALS* (e.g., *ACQSLEWY*).
   - Flight SoftWare parameters (FSW) will be in SMALL CAPITALS. All TA FSW patchable constants begin with "PCTA_" (e.g., PCTA_CALTARGETOFFSET). In this ISR, this prefix is considered implied after the initial introduction of a paramater, and will not always be included. FSW patchable constants relating to mechanism positions begin with PCMECH_ and will always be included in references.
   - Archived COS files are in FITS (.fits) format. FITS filenames, or portions of a filename, will be in sans-serif (e.g., ld9mg2nrq_rawtag.fits or _spt.fits). COS filenames are in the form IPPPSSOOT_*extension*.fits. The HST naming convention breaks down for COS as I=Instrument="L", PPP=Program ID, SS=Visit ID, OO=Exposure ID, and T="Q" for nominally recorded observations. See the COS DHB for a full breakdown of the HST IPPPSSOOT naming conventions. COS TA files have the *extension* of rawacq, and additional information useful for TA analysis is contained in the IPPPSSOOT_*spt*.fits files known as the support file, and in the IPPPSSOOT_*jit/f*.fits file known as the jitter files.

5. COS contains numerous FUV and NUV central wavelength settings, which are defined in the FSW by the OSM1 or OSM2 rotation positions. In this ISR, the term *CENWAVE*, which is also the FITS keyword name, will be used to mean any of the pre-defined OSM1 + OSM2 rotation settings that uniquely define a central wavelength setting.

6. COS *CENWAVE*s are named for the (predicted) lowest wavelength that lands on the FUVA detector segment for *FP-POS*=3. For convienence, when referring to a specific *CENWAVE* we will either call out the grating and *CENWAVE* is use as GRATING/*CENWAVE* (e.g. G130M/1222), or just use a leading "C" to identify a particular *CENWAVE* (e.g., C1222) in the same manor as "G" is used for GRATING (e.g., G130M). Note that the FITS header keyword equivalent of GRATING is *OPT_ELEM*.

7. Unless specified, all spectroscopic exposures were taken at *FP-POS*=3.

8. When referring to an HST program number, we will use either "HST PID" or a leading "**P**" in a similar fashion an "C=*CENWAVE* " and "G=GRATING", but using a **bold** font.

9. The COS FUV detector has two independent segments, Segment-A and Segment-B. In this ISR, they will be referred to as FUVA & FUVB.

10. `ACQ/IMAGE` can use either of two "MIRROR" modes, MIRRORA or MIRRORB. In this ISR, they will be referred to as MIRA & MIRB.

11. Following the conventions used in APT and the Phase II Proposal Instructions (Rose et al., 2017), NUV `ACQ/PEAKXD` exposures will specify which `STRIPE`[1] is used during TA. In this ISR, we will always use the default (`STRIPE=DEF`) for a given *CENWAVE* . This default is `STRIPE=MEDIUM` (or STRIPE=B) for all *CENWAVE*s , except G230L/3360 where it is `STRIPE=SHORT` (STRIPE=A).

12. When referring to a particular day, we will use YEAR.DAY. For example, day 60 of 2010 will be referred to as 2010.060. We will also occasionally use decimal years. In these cases, there will only be a single digit in the fractional part (e.g., 2009.9).

13. HST observations are grouped in approximately annual "cycles". 'C##' will be used as shorthand for "HST Cycle ##" (e.g., Cycle 19 = C19).

14. Unit abbreviations:

    - Milli-arcseconds (0.001″) will be abbreviated as mas.
    - Milli-amperes (0.001A) will be abbreviated as mA.
    - Counts per second will be abbreviated as cps.

15. COS has two internal PtNe wavelength calibrations lamps that send light through the Wavelength Calibration Aperture (WCA) and onto the detectors.The two PtNe lamps are referred to in this ISR as P1 and P2. Each lamp has three current settings, LOW, MEDIUM (MED) or HIGH. The P1 lamp is used for spectroscopic lamp flashes during science exposures ("TAGFLASH"es), while the P2 lamp is used for all TA exposures. Both lamps have MED current settings of 10 mA, but the P1 lamp has LOW/HIGH current setting of 6/18 mA. The P2 lamp has LOW/HIGH current settings of 3/14 mA. COS Lamp output generally scales as current$^2$ ($P = I^2 R$).

16. STScI uses a problem reporting (PR) system to track HST changes. Where applicable, these STScI PR identifying numbers will be included with *PR##*.

17. Each COS `ACQ/` mode calls one or more FSW routines which interact with HST+COS to perform the TA. The FSW routine names begin with LTALTA. The FSW routines called by each `ACQ/` mode are given in Table **??**.

18. We use the FSW NUV imaging plate scales values of 0.02352″/p (AD) and 0.02362″/p (XD)[2] as these are in agreement with the SMOV results of Goudfrooij et al., 2010. We also assume the NUV detector orientation as described in Goudfrooij et al., 2010 (a 0.52° rotation between the NUV detector coordinates and the APT POS_TARG system).

[1] `STRIPE` is the optional parameter name in APT, therefore the `Courier` font is used.

[2] The C25 COS IHB (Fox et al., 2017) does not differentiate between AD and XD NUM imaging plate scales, and lists 0.0235 "/p for both AD and XD.

## 1.2 ISR Organization

In § **??** we will discuss the concepts involved in the TA monitoring strategy along with a basic review of COS TA operations and centering requirements (§ **??**). In § **??** we will discuss the details of the individual COS TA monitoring programs and, in § **??** list the individual exposures. Also in this section, we will discuss the annual HST FGS-to-SI alignment programs and there connection to the COS TA monitoring programs (§ **??**).

In § **??**, we discuss the numerous detector subarrays used in COS TA, and their verification by the programs in this ISR.

In § **??** we will discuss the verification of the FSW parameters, lamp operations, and subarrays associated with COS `ACQ/IMAGE`s.

In § **??**, we will discuss the verification of the FSW parameters, lamp operations, and subarrays associated with COS spectroscopic TAs.

## 1.3 COS TA Monitoring Program History

After the installation of COS into HST in 2009 (STS-125), and the servicing mission orbital verification (SMOV) phase, a series of calibration programs in NUV imaging mode carefully determined the two-dimensional offset from the COS WCA to the center of the PSA when observed with MIRA. These X and Y offsets were loaded in the FSW TA parameters XIMCALTARGETOFFSET and YIMCALTARGETOFFSET. A target was then centered using a PSA×MIRA `ACQ/IMAGE`, and a target image was taken along with a MIRB image of the WCA image. These images were used to determine the AD (Y) and XD (X) offsets of the image target and WCA centroids. These values were uploaded in the FSW paramaters. This bootstrapping procedure was repeated with the BOA×MIRA and BOA×MIRB `ACQ/IMAGE` modes until all four `ACQ/IMAGE` modes were co-aligned.

The FGS-to-SI programs perform a PSA×MIRA `ACQ/IMAGE` on a target that should be ≈ centered in the aperture. After some post-processing analysis of the spacecraft telemetry, the PSA×MIRA `ACQ/IMAGE` can be used to estimate the accuracy of the NUV PSA aperture position in the SIAF[3].

## 1.4 COS centroid measurements

The COS FSW uses either a mean or a median to calculate spectral XD locations and imaging wavelength lamp center centers. On the NUV channel, medians are always used, while for FUV, a mean is always used. This behavior is controlled by the following FSW patchable constants[4] :

1. **pcta_UseMedian4CAL4FUV**

   Description: Flag to indicate whether to use "median" or "mean" for the calculation of the cross-dispersion coordinate of the wavelength calibration lamp spectrum in the phase `LTACAL` for the FUV detector.

   Format: Boolean

[3]Science Instrument Aperture File (Mallo, 2008)

[4]"Current Value" indicates the LV61 value. These values have worked well and there is no reason to consider changing these values at this time.

Units: None

Limits/Ranges: TRUE = use median; FALSE = use mean

Scaling: None

Current Value : FALSE (use mean)

2. **pcta_UseMedian4CAL4NUV**

   Description: Flag to indicate whether to use 'median' or 'mean' for the calculation of the cross-dispersion coordinate of the cal lamp spectrum in the phase `LTACAL` for the NUV detector.

   Format: Boolean

   Units: None

   Limits/Ranges: TRUE = use median; FALSE = use mean

   Scaling: None

   Current Value : TRUE (use median)

3. **pcta_UseMedian4PKXD4FUV**

   Description: Flag to indicate whether to use 'median' or 'mean' for the calculation of the cross-dispersion coordinate of the target spectrum in the phase `LTAPKXD` for the FUV detector.

   Format: Boolean

   Units: None

   Limits/Ranges: TRUE = use median; FALSE = use mean

   Scaling: None

   Current Value : FALSE (use mean)

4. **pcta_UseMedian4PKXD4NUV**

   Description: Flag to indicate whether to use 'median' or 'mean' for the calculation of the cross-dispersion coordinate of the target spectrum in the phase `LTAPKXD` for the NUV detector.

   Format: Boolean

   Units: None

   Limits/Ranges: TRUE = use median; FALSE = use mean

   Scaling: None

   Current Value : TRUE (use median)

The COS aperture mechanism is only repeatable in the XD direction to $\pm 1$ motor step (0.053″). In addition, the WCA location phase of the `ACQ/IMAGE` (*LTAIMCAL*), which uses the median integer pixel location as the lamp location, cannot measure the WCA position to better than $\frac{1}{2}$ pixel in either AD or XD. On the NUV detector, an imaging pixel is $\sim$ 0.02352″(AD) and $\sim$ 0.02362″(XD), so there is an intrinsic radial uncertainty of $\sim$0.017″after each *LTAIMCAL*.

The target location phase of `ACQ/IMAGE` (`LTAIMAGE`) uses a flux-weighted centroid over a 9×9 checkbox, which is described in detail in the COS IHB (C25, Fox et al., 2017: Section 8.4, "ACQ/IMAGE Acquisition Mode") and in § 4.2 of COS TIR 2010-03 (Penton & Keyes, 2010). A point source in a PSA×MIRA image produces an approximately Gaussian image with a FWHM of 2.5p. The 9×9 checkbox considers the majority of the target ($>$ 70%[5]) light while minimizing background contamination,[6] and should find the target center to within $\pm\frac{1}{3}$p.

[5] The PSA×MIRB, BOA×MIRA, and BOA×MIRB 9×9 checkbox fractions are ≈ 51%, 38%, and 28%, respectively.

[6] As of April, 2018, the average NUV detector background was ≈ 8.2E-4 counts/s/p.

During TA, all `ACQ/` procedures operate in ACCUM mode (no individual photon events, no pulse-height information, and no calibrations available) and operate using integer values only. For `ACQ/IMAGE`, the WCA lamp image location is determined using a median in each coordinate. Therefore, a ± 0.5p uncertainty is present during each `LTAIMCAL` measurement when determining the center of the SA position for the `LTAIMAGE` portion of the `ACQ/IMAGE`. For NUV `ACQ/PEAKXD`, the same ± 0.5p uncertainty is present in both the spectral and target locations portions of the `LTAPKXD`. Combined in quadrature, this implies that an `LTAPKXD` has an inherent XD centering accuracy of no less than $\sqrt{(2)}$ 0.5 p = 0.7p = 0.017″. For FUV `LTAPKXD`, a mean is used to measure both the WCA lamp spectrum XD location and the target XD location. For FUV LP1–3, uncorrected geometric and thermal distortions can cause targets with different spectral energy distributions (SEDs) to center differently. This effect has been measured (Penton & Keyes, 2010) to be as large at $\pm 2$ DE (rows) or $\sim 0.2''$.[7]

[7] At FUV LP4 this effect is even more pronounced and prohibits `LTAPKXD` (`NUM_POS=1ACQ/PEAKXD`) from achieving the centering requirement of $\pm 0.3''$. For this reason, the `ACQ/PEAKD` FSW routine `LTAPKD` was enabled for XD usage in FSW version LV58 (installed 2014.132).

# 2 COS TA Operations Summary

There are three modes of Target Acquisition (TA) for the Cosmic Origins Spectograph (COS); NUV imaging, NUV spectroscopic, and FUV spectroscopic. There are four COS TA (ACQ/) procedures; ACQ/IMAGE, ACQ/PEAKD, ACQ/PEAKXD, and ACQ/SEARCH. ACQ/PEAKD and ACQ/SEARCH step the telescope through dwell patterns on the sky. As long as the target light falls correctly within the TA detector sub-arrays, ACQ/PEAKD and ACQ/SEARCH will continue to nominally assist in TA (barring any unforeseen anomalies, such as detector 'hot-spots'). The ACQ/IMAGE and ACQ/PEAKXD procedures also rely on the sub-arrays, but also rely on numerous patchable (changeable) constants in the COS flight software (FSW) which assist in target centering.

In both ACQ/IMAGE and ACQ/PEAKXD, the internal wavelength calibration lamp is flashed to locate the center of the wavelength calibration aperture (WCA). From this location, the center of the science aperture (SA) in use, which could be the PSA or BOA, can be predicted by applying the FSW constants that give the SA offset compared to the WCA center. For ACQ/IMAGE, the offset is in both detector 'X' (along-dispersion, AD) and 'Y' (cross-dispersion, XD). For ACQ/PEAKXD, which uses dispersed light, this offset is only in the Y (XD) direction. All programs verify that the TA subarrays in use for the given cycle were proper for the ACQ/modes tested, verify that the actively used WCA-to-SA offsets, and monitor, as much as possible, the performance of COS TAs.

To combat the effects of FUV gain sag, the FUV ACQ/PEAKXD algorithm was modified in C19 to only use the FUVA segment. All FUV ACQ/PEAXKD exposures discussed in this ISR are FUVA-only. [8]

BOA spectroscopic TAs were not supported during C19–C24, accordingly the programs discussed here only verify PSA spectroscopic TAs. WCA-to-PSA offsets are used in ACQ/PEAKXDs, and each COS grating has a different XD offset. These offsets are both grating (OPT_ELEM) and lifetime position (LP) dependent.[9] The programs listed here verify the NUV LP1 as well as FUV LP2[10] and LP3[11]. The FUV LP4 uses a different ACQ/PEAKXD algorithm (NUM_POS> 1), and, like ACQ/PEAKD, does not use the WCA-to-SA XD offsets[12].

The initial HST/COS target pointing is based on definitions of the physical locations of the COS apertures in terms of [V2,V3] in the Science Instrument Aperture File (SIAF). All of the actively used NUV (LP1) and FUV LP2 and LP3. SIAF entries used for TA during C21–C24 are also verified in this program.[13]

These programs, and this ISR, do not attempt to monitor the AD accuracy of the COS spectroscopic TA modes.[14]

[8]The change went into effect on April 18, 2011 (2011.101).

[9]In the COS FSW, these WCA-to-SA XD offsets are stored in the PCTA_CALTARGETOFFSET table.

[10]The default COS FUV spectral location for all *CENWAVE*s was moved from LP1 to LP2 on July 23,2012 (2012.205).

[11]The default COS FUV spectral location was moved to LP3 on February 15, 2015 (2015.046) for all *CENWAVE*s except G130M/1055 and G130M/1096, which still operate at LP2. On October 2, 2017 (2017.275), the default FUV spectral location was moved to LP4, with additional observing and TA constraints as outlined on the COS2025 website (http://www.stsci.edu/hst/cos/cos2025).

[12]All NUV and FUV LP1-3 ACQ/PEAKXD observations use the optional parameter, NUM_POS=1.

[13]These entries are not really really tested that accurately, because ..... . .

[14]For ACQ/PEAKD, short-term fluctuations of the detector background rate due to environmental conditions remains the largest source of AD pointing error.

## 2.1 COS TA Centering Requirements

The COS TA centering requirements are based upon the wavelength accuracy requirements in the AD, and for flux and resolution optimization in the XD.[15] The strictest NUV requirements are [AD,XD] = [0.041, 0.3]″, while for the FUV they are [AD,XD] = [0.106, 0.3]″.[16] Since the AD requirement is in units of $\text{km s}^{-1}$, it is detector, grating, and wavelength dependent as defined, generally, in Equation **??**, and specifically for each grating in Equations **??–??**. Wavelengths assigned to COS data are required to have an absolute uncertainty of less than ±15 k/ms in the medium resolution modes, ±150 km/s in G140L mode and ± 175 km/s in G230L mode. In the XD direction, the requirement is to be centered to within ±0.3″, however, our goal is ±0.1″ for FUV flat-fielding purposes. Since the AD requirement is in units of km/s, it is detector and wavelength dependent as defined and shown in Equation **??**.

$$\Delta AD(\mathring{A}) = \frac{\text{velocity requirement } \times \lambda}{c \ \times \text{dispersion } (\mathring{A}/p) \times \text{platescale } (p/'')} \tag{5}$$

$$\Delta\ AD(G185M@1825\mathring{A}) = \frac{15 \text{ km s}^{-1} \ \times 1825\mathring{A}}{c \times 0.037\mathring{A}/p \times 42.47p/''} = 0.058'' \tag{6}$$

$$\Delta\ AD(G225M@2250\mathring{A}) = \frac{15 \text{ km s}^{-1} \ \times 2250\mathring{A}}{c \times 0.035\mathring{A}/p \times 42.47p/''} = 0.076'' \tag{7}$$

$$\Delta\ AD(G285M@2850\mathring{A}) = \frac{15 \text{ km s}^{-1} \ \times 2850\mathring{A}}{c \times 0.040\mathring{A}/p \times 42.47p/''} = 0.084'' \tag{8}$$

$$\Delta\ AD(G230L@2450\mathring{A}) = \frac{175 \text{ km s}^{-1} \ \times 2450\mathring{A}}{c \times 0.390\mathring{A}/p \times 42.47p/''} = 0.086'' \tag{9}$$

$$\Delta\ AD(G130M@1300\mathring{A}) = \frac{15 \text{ km s}^{-1} \ \times 1300\mathring{A}}{c \times 0.00997\mathring{A}/p \times 43.5p/''} = 0.150'' \tag{10}$$

$$\Delta\ AD(G160M@1600\mathring{A}) = \frac{15 \text{ km s}^{-1} \ \times 1600\mathring{A}}{c \times 0.01223\mathring{A}/p \times 42.9p/''} = 0.153'' \tag{11}$$

$$\Delta\ AD(G140L@1800\mathring{A}) = \frac{150 \text{ km s}^{-1} \ \times 1800\mathring{A}}{c \times 0.08030\mathring{A}/p \times 45.4p/''} = 0.247'' \tag{12}$$

Assuming that the wavelength error budget is split evenly between the COS TA and wavelength scale accuracies, the error budgets for the COS gratings, in arc-seconds (″), are given in Table **??**. By "evenly" we mean that when added in quadrature the total error budget is that given by the second column of Table **??**. Setting the TA error budget equal to the wavelength scale accuracy, the AD TA requirement given in the third column is the second column divided by $\sqrt{2}$.

[15] The COS requirements are documented in the CEI (Contract End Item) Specification (Smith et. al., 2004).

[16] While the XD requirement for all TAs is ± 0.3″, our $1\sigma$ goal is ± 0.1″. This goal ensures that spectra fall on a consistent XD location on the the detector, which aids in extraction and calibration accuracy.

Table 1. COS TA Centering Requirements

| *OPT_ELEM* | Total AD Error Budget | AD TA Requirement[a] | XD TA Requirement[x] |
|---|---|---|---|
| | | NUV | |
| G185M | 0.058″ | 0.041″ | 0.3(0.1)″ |
| G225M | 0.076″ | 0.054″ | 0.3(0.1)″ |
| G285M | 0.084″ | 0.059″ | 0.3(0.1)″ |
| G230L | 0.086″ | 0.061″ | 0.3(0.1)″ |
| | | FUV | |
| G130M | 0.150″ | 0.106″ | 0.3(0.1)″ |
| G160M | 0.153″ | 0.108″ | 0.3(0.1)″ |
| G140L | 0.247″ | 0.175″ | 0.3(0.1)″ |

[a]Assuming the total AD error budget (column 2) is split equally between TA centering and wavelength scale accuracy, the AD TA requirements (column 3) are $1/\sqrt{2}$ of the total AD error budget (equations **??**–**??**).

[x]The XD requirement is 0.3″, but our $1\sigma$ goal is 0.1″.

# 3 Program Descriptions

COS ACQ/IMAGE has four commonly used combinations of two Science Apertures (SAs), the Primary Science Aperture (PSA) and the Bright Object Aperture (BOA), and two mirror modes, MIRA and MIRB. During the 2009 servicing mission orbital verification (SMOV) phase, a series of C17 calibration programs in NUV imaging mode (**P**11469, **P**11473, & **P**11471) carefully determined the two-dimensional offset from the COS WCA to the center of the PSA when observed with MIRA. These X and Y offsets were loaded in the FSW TA parameters[17]. A target was then centered using a PSA+MIRA ACQ/IMAGE, then a target image was taken along with a MIRB image of the WCA image. These images were used to determine the AD (Y) and XD (X) offsets of the image target and WCA centroids. These values were uploaded in the FSW paramaters. This bootstrapping procedure was repeated with the BOA+MIRA and BOA+MIRB ACQ/IMAGE modes until all four ACQ/IMAGE modes were co-aligned.

In the COS TA Monitoring programs described in this ISR, we re-use this bootstrapping strategy to test the co-alignment of all four ACQ/IMAGE modes[18]. In addition to COS calibration programs listed above, and described in detail is § **??–??**, COS ACQ/IMAGE exposures obtained in numerous cycles of the "Focal Plane Calibration (SI-FGS Alignment)" series were used in the COS TA monitoring discussed in this ISR. These programs were developed by the HST Telescope's division (PIs Cox and/or Lallo) for Fine Guidance Sensor (FGS) to Science Instrument (SI) alignment, and are described in § **??**.

All data for a given cycle were intentionally taken contemporaneously to avoid any long-term detector or spacecraft effects from affecting our results. Our requirement was that all data for a given program were taken within 45 days of each other. There were minor differences in the specific exposures in each cycles TA monitoring program, these are discussed in § **??**.

## 3.1 FGS-to-SI Programs

From C17–C23, an FGS-to-SI program executed with COS visits twice a year. These programs contained COS exposures designed to assist in the monitoring of the COS NUV alignent to HST. These programs used the same two target stars with COS in visits spaced six months apart. Both visits observed the astrometric open cluster M35, at orientations that were 180° apart. The two stars observed were 206W3 (in the Fall) and 427W3 (in the Spring). Due to time constraints, the exact content of the COS visits in these programs varied from year to year.

However, the COS portion of each program begins with a PSA×MIRA ACQ/IMAGE on a target should be approximately centered due to observations with other instruments earlier in the visit. Post-observation telemetry data, an the results of the ACQ/IMAGE, are used to refine this assumption. This process verifies the COS NUV PSA aperture position[19] in the SIAF to about 0.5 pixels or ( 0.012″).

[17] In the COS FSW, these WCA-to-SA offsets are stored as patchable constants in the PCTA_XIMCALTARGETOFFSET (XD) and PCTA_YIMCALTARGETOFFSET (AD)

[18] The underlying assumption of these programs is that that the PSA/MIRA ACQ/IMAGE centering has not changed since SMOV.

[19] Specifically, the *LFPSAA* SIAF entry.

Table 2. Historical List of FGS-to-SI proposals used for COS TA Monitoring.

| PID | Cycle | Summary of Contents |
|---|---|---|
| **P**11878 | C17 | 2 sets of PSA ACQ/IMAGEs, Target+Lamp TT images, & G230L Spectra |
| **P**12399 | C18 | 2 sets of PSA ACQ/IMAGEs, 1 set of Target+Lamp TT images + G230L Spectrum (427W3) |
| **P**12781 | C19 | 2 sets of PSA ACQ/IMAGEs |
| **P**13171 | C20 | 2 sets of PSA ACQ/IMAGEs |
| **P**13616 | C21 | 2 sets of PSA ACQ/IMAGEs |
| **P**14035 | C22 | 2 sets of PSA ACQ/IMAGEs |
| **P**14452 | C23 | 2 sets of PSA ACQ/IMAGEs, with Lamp-Only TT images after each ACQ/IMAGE |

After this PSA×MIRA ACQ/IMAGE, a PSA×MIRB ACQ/IMAGE is then performed (together, a "set"). This bootstraps the PSA×MIRB centering to the PSA×MIRA and to the SIAF verification. This allows us to monitor the properties of the PSA×MIRB image in a controlled way on a centered target.

The historical list of FGS-to-SI proposals, HST cycles (C##), and content are given in Table **??**. Where possible, time-tag (TT) images of the lamps and/or targets, along with NUV G230L spectra were acquired.

## 3.2 COS TA Monitoring Program Structure

Each cycles TA monitoring program contains three single-orbit visits. The number of visits is mandated by the bootstrapping technique between the four different ACQ/IMAGE SA×MIR combinations.

Each visit begins with a comparison of the centering of two ACQ/IMAGE modes out of the possible four science apertures (SA, PSA or BOA) × (MIRA or MIRB). This back-to-back ACQ/IMAGE process allows us to test that all ACQ/IMAGE modes are centering the target to the same point in the aperture. This comparison involves not only the ACQ/IMAGEs, but NUV detector images of the PtNe lamp (WCA) image and, if possible, coeval target images. These direct lamp+target comparisons are only available for the PSA modes. For the BOA modes, the WCA lamp images and target images are taken consecutively. The lamp+target exposures are interleaved throughout the visit to measure and verify the imaging WCA-to-SA offsets are still accurate for each HST Cycle. Images will usually use the PtNe#2 (P2) lamp, as it is the primary TA lamp, but some images will use PtNe#1 (P1) to monitor both lamps in imaging mode.

In its generic format, the three, one-orbit, visits are configured as follows:

- The first orbit on each program is designed to test the co-alignment of the PSA×MIRA and PSA×MIRB ACQ/IMAGE combinations. However, this exact combination of ACQ/IMAGEs occurs at the end of each semi-annual visit in the FGS-to-SI alignment programs (see § **??**). This visit was usually treated as an on-hold contingency visit in case, for whatever reason, the fall visit of the program did not execute in a given cycle.[20] The target for this contigency

[20]Beginning with Cycle 23, this program was replaced with an improved process for aligning the FGSs. Accord-

visit is 206W3, the same target as the Fall visit of the FGS-to-SI alignment program. As discussed further in § **??**, in one case, (C22, **P**13972), this visit was re-purposed to verify a change to the MIRB`ACQ/IMAGE` configuration required due to the increasing background (see § **??**).

- The second orbit of each program takes back-to-back PSA×MIRB and BOA×MIRA `ACQ/IMAGE`s and target (WD1657+343) TIME-TAG images (with lamp flashes). A second PSA×MIRB `ACQ/IMAGE` is then performed to provide a second measurement of the offset. Additionally, NUV and FUV spectra are acquired to test their WCA-to-PSA offsets.
- The third orbit of each program takes back-to-back BOA×MIRA and BOA×MIRB `ACQ/IMAGE`s and target (HIP66578) TIME-TAG images (with lamp flashes). As in the second orbit, a second BOA×MIRA `ACQ/IMAGE` is then performed to provide a second measurement of the offset. Additional NUV and FUV spectra are acquired to the remaining WCA-to-PSA offsets not tested in the second orbit.
- All visits were executed in APT 3-Gyro mode (`3GOBAD`) with the `BASE1B3` guide star requirement set in APT.

The exact configuration of which gratings and which *CENWAVE*s were spectroscopically tested varied with each cycle as the programs evolved. Specifically, with the 2015 change in OSM2 home position[21], NUV spectra were re-ordered for efficiency and some NUV *CENWAVE*s were changed to those that are known to have strong *STRIPE*=B WCA spectra against the increasing detector background (Fix, 2018) and declining NUV sensitivity (Taylor, 2017). In C23–C24, we took G160M/1600 exposures offset in XD by $\pm 0.7''$[22] to test for the effects of Ywalk on FUV spectra at LP3. In addition, one visit of each program, usually the second visit, performed an annual "family portrait" of all the P1/P2 MIRA/B WCA lamp images to track any drifting of the centroids, or changes in the lamps with time. Further details on the differences between the programs is provided in § **??**.

## 3.3 Differences between HST+COS TA monitoring programs

There are several important differences between the various versions of the COS TA monitoring programs:

- In the initial, C20, version of the TA monitoring program (**P**13124), the PSA×MIRB + BOA×MIRA `ACQ/IMAGE` visit ('01', 24-Oct-2013), contained G230L/3000, G285M/2850, G130M/1309 & G140L/1280. The BOA×MIRA + BOA×MIRB `ACQ/IMAGE` visit ('02', 01-Nov-2013) contained G185M/1890, G225M/2306, and both BOA and PSA G160M/1623 spectra. A 2×2 `ACQ/SEARCH` proceeded the BOA×MIRA `ACQ/IMAGE` in visit '02' due to some uncertainty in the rather large ($>400$ mas/yr) proper motion of the target (HIP66578).

ingly, we activated this contingency visit to obtain the necessary PSA×MIRA and PSA×MIRB exposures.

[21] In May 2015, the "home" position of the COS Optic Select Mechanism #2 (OSM2, the NUV grating wheel) was changed from G185M/1850 to the MIRA position to reduce wear on the OSM, increase observing efficiency, and reduce mechanism drift and position offsets during `ACQ/IMAGE` TAs. (see HST *PR*#80893 and *PR*#80894).

[22] Offsets set by using APT exposure level *POS_TARG*s.

- In the C21 TA monitoring program (**P**13526), the a 2×2 `ACQ/SEARCH` present in the beginning of Visit '02' was removed after further verification of the proper motion. Also, the G160M BOA spectrum was dropped in favor of the $\pm 0.7''$ `POS_TARG` exposures to monitor gain sag/Ywalk at LP2 in Visit '02' (17-Nov-2014). In addition, a 'family portait' of the P1 and P2 PtNe lamps were acquired using both MIRA and MIRB NUV imaging. The MIRA lamp images were taken for both the P1 and P2 lamps at LOW current, while for MIRB image the P1 lamp image was taken at LOW current and the P2 lamp was at MED current. Additionally, the C21, **P**13526, contingency visit '03' was activated to verify the count rates associated with the re-configuration of the the MIRB `ACQ/IMAGE` lamp flash of the MIRB `LTACAL` exposures for P2 from LOW to MED current. All MIRB lamp images in the C21 program were also taken at MED current, as compared to LOW for the C20 program. Further details on the MIRB `ACQ/IMAGE` adjustments are given in § **??**.

  The optional parameter `WAVECAL=YES` in the BOA×MIRA target+Lamp image of the C20 program was discovered to not have taken the expected internal lamp image expected in the LC6601RYQ_rawtag.fits exposure. Correcting this inconsistency would have required significant APT, TRANS, and commanding changes. As this internal calibration exposure combination is rarely executed, the C21 program included separate `TARGET=WAVE` companion lamp exposures for the target BOA exposure[23] A second MIRA lamp image was added directly after the BOA×MIRA `ACQ/IMAGE`, to verify the repeatability of the WCA lamp location when moving the BOA into and out of position. To create time for the new exposures, the exposure times of the spectroscopic observations were scaled back, but still achieved the required S/N to measure the XD spectral locations.

- In the C22 TA monitoring program (**P**13972), the G185M and G285M exposures were changed from C2850 to C2676 and from C1890 to C1913, respectively, as the WCA lamp spectra much stronger in the latter `STRIPE=B` bandpasses. Beginning with C22, GOs were discouraged from using the G285M for spectroscopic PEAKXD TAs, and the *CENWAVE*s for the other NUV gratings were highlighted in section 2.6 (NUV Spectroscopic Acquisitions) of the C25 COS Instrument Handbook (Fox, 2017) and C25 Phase II Proposal Instructions (Rose, et al., 2017). Prior to C25, GOs were contacted directly by their Contact Scientists (CS) to ensure the success of their NUV spectroscopic `ACQ/PEAKXD`s. The contingency visit ('03') was not executed in C22.

- In the C23 TA monitoring program (**P**14440), each of the one-orbit visits was placed in a non-interruptable sequence to prevent guide-star (GS) re-acquisitions (reacqs) from changing the telescope pointing during a visit. None of the previous visits encountered this situation, but the use of the non-interruptable sequences in APT requires this to be true for this, and all all subsequent programs. The lamp 'family portrait' in Visit '02' is contained in a separate non-interruptable sequence from the other exposures in the visit as any GS reacqs would not affect the internal lamp exposures. Some exposures were slightly lengthened

[23] The COS apertures are physically configured such that WCA light lands on the detector(s) when the PSA in place, but does not when the BOA is in place (INSERT REF). Therefore, whenever lamp images are required to verify BOA `ACQ/IMAGE` exposures, the BOA is replaced by the PSA so that WCA light falls on the detector at the same location as it would fall for a PSA image.

to take advantage of the increased efficiency of the modified OSM2 home position.[24] The contingency visit ('03') was not executed in C23.

- In the C24 TA monitoring program (**P**14857), the visit names were changed from '01', '02', and '03' to 'BA', 'BB', and 'PB' to indicate which `ACQ/IMAGE` mode was being tested; PB = PSA×MIRB, BA = BOA×MIRA, and BB = BOA×MIRB. Visits 'BA' and 'BB' of the C24 program are identical to visits '01' and '02' of the C23 program in all other regards. Visit 'PB' of the C24 program is noticeably different than the contingency visit '03' in C23 program. The 'PB' visit only includes those exposures absolutely required to compare the `ACQ/IMAGE` accuracy of PSA×MIRA to PSA×MIRB, while the C23 program also obtained spectra of all three FUV gratings for additional monitoring of spectroscopic TA performance under the assumption that detector 'Y-walk' monitoring would benefit from additional observations near the end of the FUV LP3 lifetime. As all three visits of 14857 executed near the end of the LP3 lifetime, these additional exposures were not required. The C24 version of the FGS-to-SI program was replaced with an improved program (**P**14867[25]) for aligning the FGSs which did not allow the inclusion of these `ACQ/IMAGE` exposures[26]. For C24, we activated this visit to obtain the needed PSA×MIRA to PSA×MIRB `ACQ/IMAGE` alignment verification.

## 3.4 Exposure Lists

Table **??** gives the operational details of all NUV imaging exposures which opened the external shutter used in this ISR. Table **??** gives the operational details of all NUV imaging WAVECAL exposures Tables **??** and **??** give the details of all spectroscopic exposures used in this ISR. All tables follow the convention that if an entry was extracted from a FITS header, then the column name will appear in *ITALICIZED ALL CAPITALS*.

The columns of the Table **??** give:

1. *ROOTNAME* gives the IPPPSSOOT of the COS exposure,
2. *PROPOSID* gives the HST program id (PID),
3. *TARNMAME* gives the target name as present in the MAST archive,
4. *OBSMODE* gives the observation mode, where "TT" is used for Time-Tag observations,
5. *EXPTYPE* gives the exposure type, which is either `ACQ/IMAGE` or EXT/SCI. *APERTURE* = PSA EXT/SCI images allow co-eval target and lamp images for direct measurement of their WCA-to-SA offset. `ACQ/IMAGE` exposures return before and after target images in OBSTYPE=ACCUM, but do not return lamp images.
6. *EXPTIME* gives the exposure time in seconds. For EXT/SCI PSA images, the lamp time may be different. These lamp times are given in Table **??**.
7. PtNe Lamp# gives the wavelength calibration lamp name, P1 or P2.
8. Lamp Current gives the lamp current setting. The conversion from current setting to current in milli-amps (mA) is given in § **??**, and in the table footnotes.

[24]The OSM2 home position was changed from G185M to MIRA on July 6, 2015 (2015.157).
[25]HST Cycle 24 Focal Plane Calibration (SI-FGS alignment), PI = Edmund Nelan.
[26]The FGSs were used as the prime science instrument in this proposal, which precluded the use of COS during the visit as COS is not an allowed parallel HST instrument.

9. *APERTURE* gives the COS SA (PSA or BOA).
10. *OPT_ELEM* gives the grating or MIRROR used as the primary optic.
11. *APERXPOS* gives the AD (X in detector coordinates) aperture position. The default position is *APERXPOS*=22 for all FUV and NUV science and TA exposures.[27]
12. *APERYPOS* gives the XD (Y in detector coordinates) aperture position. It is not uncommon that the XD aperture location (*APERYPOS*) is $\pm$ one step off from its nominal position. Each *APERYPOS* step is $\approx 0.05''$, or about $\frac{1}{6}$ of our XD centering requirement, and $\frac{1}{2}$ of our $1\sigma$ XD centering goal. The default NUV and FUV LP1 PSA/BOA positions are *APERYPOS*=$126/-153$, where the WCA has the same XD (*APERYPOS*) position as the PSA. As shown in Table **??** the nominal PSA & WCA *APERYPOS* position for LP2, LP3, and LP4 are +53, +181, and +234, respectively.[28]
13. *DATE-OBS* gives the date of the observation in YEAR-MOnth-DAy format.

The columns of the spectroscopic NUV (Table **??**) and FUV (Table **??**) tables are similar to the columns listed above for Table **??**, with the following exceptions:

- All spectroscopic exposures are with the PSA, so the *APERTURE* column has been removed.
- The “Lamp#” and “Lamp Current” columns are not present. In the programs of this ISR, the default P1 lamp usage for spectroscopic observations was overridden with the use of the USELAMP=LINE2 and CURRENT=MEDIUM special commanding in APT to simulate the lamp exposures obtained in `NUM_POS=1ACQ/PEAKXD` (`LTAPKXD`) exposures. In addition, the APT optional parameter FLASH was used to set P2 exposures times that provided counts in excess of those expected during the TA exposures. Since all spectra were taken in TT mode, if required, an exact replica of the counts received in an actual `LTAPKXD` WCA spectrum could be re-produced. The additional counts allow for a better determination of the WCA-to-PSA XD offsets discussed in § **??** and § **??**.
- The *OPT_ELEM* column shows the grating in use, as this in now the primary optic.
- The column *CENWAVE* now follows the *OPT_ELEM* column, and gives the central wavelength setting of the exposure.
- The *LIFE_ADJ* column (LP) gives the lifetime position of the observation. Note that there is only one NUV LP, so all observations are LP1.

[27] The trailing ”0.1” reported in the FITS headers is a conversion anomaly that is present in all aperture positions (*APERXPOS* & *APERYPOS*).

[28] As explained in the TA enabling ISRs for each FUV LP, due to known behavior of the COS aperture mechanism to miss by one step in *APERYPOS*, entries in the PCMECH_APMXDISPPOSITION FSW table were intentionally offset by $\pm$ on step, depending on travel direction from NUV/FUV LP1, which shared the common PCMECH_APMXDISPPOSITION (*APERYPOS*) entry of +126.

## Table 3. COS/NUV TA Monitoring Imaging Exposures - PSA or BOA

| *ROOTNAME* (1) | *PROPOSID* (2) | *TARGNAME* (3) | *OBSMODE*[t] (4) | *EXPTYPE* (5) | *EXPTIME* (s) (6) | PtNe Lamp # (7) | Lamp Current[c] (8) | *APERTURE* (9) | *OPT_ELEM* (10) | *APERXPOS*[x] (11) | *APERYPOS*[y] (12) | *DATE-OBS* (13) |
|---|---|---|---|---|---|---|---|---|---|---|---|---|
| PSA × MIRA | | | | | | | | | | | | |
| lc6ka1i1q | 13171 | 427W3 | ACCUM | ACQ/IMAGE | 60 | P2 | Low | PSA | MIRA | 22.1 | 127.1 | 2013-03-02 |
| lc6ka2imq | 13171 | 206W3 | ACCUM | ACQ/IMAGE | 60 | P2 | Low | PSA | MIRA | 22.1 | 127.1 | 2013-09-01 |
| lci4a1dcq | 13616 | 427W3 | ACCUM | ACQ/IMAGE | 60 | P2 | Low | PSA | MIRA | 22.1 | 127.1 | 2014-04-03 |
| lci4a2e3q | 13616 | 206W3 | ACCUM | ACQ/IMAGE | 60 | P2 | Low | PSA | MIRA | 22.1 | 127.1 | 2014-10-27 |
| lcgq03dbq | 13526 | 206W3 | ACCUM | ACQ/IMAGE | 15 | P2 | Low | PSA | MIRA | 22.1 | 127.1 | 2014-10-06 |
| lcgq03ddq | 13526 | 206W3 | TT | EXT/SCI | 15 | P2 | Low | PSA | MIRA | 22.1 | 127.1 | 2014-10-06 |
| lcgq03drq | 13526 | 206W3 | TT | EXT/SCI | 12 | P2 | Low | PSA | MIRA | 22.1 | 127.1 | 2014-10-06 |
| lcgq03dtq | 13526 | 206W3 | ACCUM | ACQ/IMAGE | 12 | P2 | Low | PSA | MIRA | 22.1 | 127.1 | 2014-10-06 |
| lcsla1i4q | 14035 | 427W3 | ACCUM | ACQ/IMAGE | 60 | P2 | Low | PSA | MIRA | 22.1 | 125.1 | 2015-04-14 |
| lcsla2bhq | 14035 | 206W3 | ACCUM | ACQ/IMAGE | 60 | P2 | Low | PSA | MIRA | 22.1 | 125.1 | 2015-10-02 |
| ldozpbf5q | 14857 | 206W3 | ACCUM | ACQ/IMAGE | 20 | P2 | Low | PSA | MIRA | 22.1 | 125.1 | 2017-09-10 |
| ldozpbf7q | 14857 | 206W3 | TT | EXT/SCI | 20 | P2 | Low | PSA | MIRA | 22.1 | 125.1 | 2017-09-10 |
| ldozpbffq | 14857 | 206W3 | TT | EXT/SCI | 20 | P2 | Low | PSA | MIRA | 22.1 | 125.1 | 2017-09-10 |
| ldozpbfhq | 14857 | 206W3 | ACCUM | ACQ/IMAGE | 20 | P2 | Low | PSA | MIRA | 22.1 | 125.1 | 2017-09-10 |
| PSA × MIRB | | | | | | | | | | | | |
| lc6ka1i3q | 13171 | 427W3 | ACCUM | ACQ/IMAGE | 300 | P2 | Low | PSA | MIRB | 22.1 | 127.1 | 2013-03-02 |
| lc6ka2ioq | 13171 | 206W3 | ACCUM | ACQ/IMAGE | 300 | P2 | Low | PSA | MIRB | 22.1 | 127.1 | 2013-09-01 |
| lci4a1deq | 13616 | 427W3 | ACCUM | ACQ/IMAGE | 300 | P2 | Low | PSA | MIRB | 22.1 | 127.1 | 2014-04-03 |
| lci4a2e5q | 13616 | 206W3 | ACCUM | ACQ/IMAGE | 300 | P2 | Med | PSA | MIRB | 22.1 | 127.1 | 2014-10-27 |
| lcgq01q5q | 13526 | WD-1657+343 | ACCUM | ACQ/IMAGE | 12 | P2 | Med | PSA | MIRB | 22.1 | 127.1 | 2014-11-19 |
| lcgq01q7q | 13526 | WD-1657+343 | TT | EXT/SCI | 16 | P2 | Med | PSA | MIRB | 22.1 | 127.1 | 2014-11-19 |
| lcgq01qhq | 13526 | WD-1657+343 | TT | EXT/SCI | 12 | P2 | Med | PSA | MIRB | 22.1 | 126.1 | 2014-11-19 |
| lcgq01qjq | 13526 | WD-1657+343 | ACCUM | ACQ/IMAGE | 12 | P2 | Med | PSA | MIRB | 22.1 | 126.1 | 2014-11-19 |
| lcgq03dfq | 13526 | 206W3 | TT | EXT/SCI | 160 | P2 | Low | PSA | MIRB | 22.1 | 127.1 | 2014-10-06 |
| lcgq03dhq | 13526 | 206W3 | TT | EXT/SCI | 180 | P2 | Low | PSA | MIRB | 22.1 | 127.1 | 2014-10-06 |
| lcgq03djq | 13526 | 206W3 | TT | EXT/SCI | 180 | P2 | Med | PSA | MIRB | 22.1 | 127.1 | 2014-10-06 |
| lcgq03dlq | 13526 | 206W3 | ACCUM | ACQ/IMAGE | 160 | P2 | Med | PSA | MIRB | 22.1 | 127.1 | 2014-10-06 |
| lcgq03dnq | 13526 | 206W3 | TT | EXT/SCI | 180 | P2 | Med | PSA | MIRB | 22.1 | 127.1 | 2014-10-06 |
| lcgq03dpq | 13526 | 206W3 | TT | EXT/SCI | 160 | P2 | Low | PSA | MIRB | 22.1 | 127.1 | 2014-10-06 |
| lcri01fzq | 13972 | WD-1657+343 | ACCUM | ACQ/IMAGE | 12 | P2 | Med | PSA | MIRB | 22.1 | 125.1 | 2015-10-06 |
| lcri01g1q | 13972 | WD-1657+343 | TT | EXT/SCI | 12 | P2 | Med | PSA | MIRB | 22.1 | 125.1 | 2015-10-06 |
| lcri01gcq | 13972 | WD-1657+343 | TT | EXT/SCI | 14 | P2 | Med | PSA | MIRB | 22.1 | 126.1 | 2015-10-06 |
| lcri01geq | 13972 | WD-1657+343 | ACCUM | ACQ/IMAGE | 12 | P2 | Med | PSA | MIRB | 22.1 | 126.1 | 2015-10-06 |
| lcsla1i6q | 14035 | 427W3 | ACCUM | ACQ/IMAGE | 300 | P2 | Med | PSA | MIRB | 22.1 | 125.1 | 2015-04-14 |
| lcsla2bjq | 14035 | 206W3 | ACCUM | ACQ/IMAGE | 300 | P2 | Med | PSA | MIRB | 22.1 | 125.1 | 2015-10-02 |
| ld3701gtq | 14440 | WD-1657+343 | ACCUM | ACQ/IMAGE | 13 | P2 | Med | PSA | MIRB | 22.1 | 125.1 | 2016-10-18 |
| ld3701gvq | 14440 | WD-1657+343 | TT | EXT/SCI | 16 | P2 | Med | PSA | MIRB | 22.1 | 125.1 | 2016-10-18 |
| ld3701h5q | 14440 | WD-1657+343 | TT | EXT/SCI | 16 | P2 | Med | PSA | MIRB | 22.1 | 126.1 | 2016-10-18 |
| ld3701h7q | 14440 | WD-1657+343 | ACCUM | ACQ/IMAGE | 13 | P2 | Med | PSA | MIRB | 22.1 | 126.1 | 2016-10-18 |
| ldozbadhq | 14857 | WD-1657+343 | ACCUM | ACQ/IMAGE | 13 | P2 | Med | PSA | MIRB | 22.1 | 125.1 | 2017-09-04 |
| ldozbadjs | 14857 | WD-1657+343 | TT | EXT/SCI | 16 | P2 | Med | PSA | MIRB | 22.1 | 125.1 | 2017-09-04 |
| ldozbadtq | 14857 | WD-1657+343 | TT | EXT/SCI | 16 | P2 | Med | PSA | MIRB | 22.1 | 126.1 | 2017-09-04 |
| ldozbadvq | 14857 | WD-1657+343 | ACCUM | ACQ/IMAGE | 13 | P2 | Med | PSA | MIRB | 22.1 | 126.1 | 2017-09-04 |
| ldozpbf9q | 14857 | 206W3 | TT | EXT/SCI | 220 | P2 | Med | PSA | MIRB | 22.1 | 125.1 | 2017-09-10 |
| ldozpbfbq | 14857 | 206W3 | ACCUM | ACQ/IMAGE | 220 | P2 | Med | PSA | MIRB | 22.1 | 125.1 | 2017-09-10 |
| ldozpbfdq | 14857 | 206W3 | TT | EXT/SCI | 220 | P2 | Med | PSA | MIRB | 22.1 | 125.1 | 2017-09-10 |
| BOA × MIRA | | | | | | | | | | | | |
| lcgq01q9q | 13526 | WD-1657+343 | TT | EXT/SCI | 150 | P2 | Med | BOA | MIRA | 22.1 | -153.1 | 2014-11-19 |
| lcgq01qdq | 13526 | WD-1657+343 | ACCUM | ACQ/IMAGE | 150 | P2 | Low | BOA | MIRA | 22.1 | -153.1 | 2014-11-19 |
| lcgq02hmq | 13526 | HIP66578 | ACCUM | ACQ/IMAGE | 12 | P2 | Low | BOA | MIRA | 22.1 | -153.1 | 2014-11-17 |
| lcgq02i0q | 13526 | HIP66578 | ACCUM | ACQ/IMAGE | 12 | P2 | Low | BOA | MIRA | 22.1 | -153.1 | 2014-11-17 |
| lcri01g3q | 13972 | WD-1657+343 | TT | EXT/SCI | 150 | P2 | Med | BOA | MIRA | 22.1 | -153.1 | 2015-10-06 |
| lcri01g7q | 13972 | WD-1657+343 | ACCUM | ACQ/IMAGE | 150 | P2 | Low | BOA | MIRA | 22.1 | -153.1 | 2015-10-06 |
| lcri02h8q | 13972 | HIP66578 | ACCUM | ACQ/IMAGE | 12 | P2 | Low | BOA | MIRA | 22.1 | -153.1 | 2015-10-06 |
| lcri02hmq | 13972 | HIP66578 | ACCUM | ACQ/IMAGE | 12 | P2 | Low | BOA | MIRA | 22.1 | -153.1 | 2015-10-06 |
| ld3701gxq | 14440 | WD-1657+343 | TT | EXT/SCI | 150 | P2 | Med | BOA | MIRA | 22.1 | -153.1 | 2016-10-18 |
| ld3701h1q | 14440 | WD-1657+343 | ACCUM | ACQ/IMAGE | 150 | P2 | Low | BOA | MIRA | 22.1 | -153.1 | 2016-10-18 |
| ld3702mzq | 14440 | HIP66578 | ACCUM | ACQ/IMAGE | 16 | P2 | Low | BOA | MIRA | 22.1 | -153.1 | 2016-10-19 |
| ld3702nhq | 14440 | HIP66578 | ACCUM | ACQ/IMAGE | 16 | P2 | Low | BOA | MIRA | 22.1 | -153.1 | 2016-10-19 |
| ldozbadlq | 14857 | WD-1657+343 | TT | EXT/SCI | 150 | P2 | Med | BOA | MIRA | 22.1 | -153.1 | 2017-09-04 |
| ldozbadpq | 14857 | WD-1657+343 | ACCUM | ACQ/IMAGE | 150 | P2 | Low | BOA | MIRA | 22.1 | -153.1 | 2017-09-04 |
| ldozbbleq | 14857 | HIP66578 | ACCUM | ACQ/IMAGE | 16 | P2 | Low | BOA | MIRA | 22.1 | -153.1 | 2017-09-06 |
| ldozbblsq | 14857 | HIP66578 | ACCUM | ACQ/IMAGE | 16 | P2 | Low | BOA | MIRA | 22.1 | -153.1 | 2017-09-06 |
| BOA × MIRA | | | | | | | | | | | | |
| lcgq02hqq | 13526 | HIP66578 | TT | EXT/SCI | 181 | P2 | Low | BOA | MIRB | 22.1 | -153.1 | 2014-11-17 |
| lcgq02huq | 13526 | HIP66578 | ACCUM | ACQ/IMAGE | 181 | P2 | Med | BOA | MIRB | 22.1 | -153.1 | 2014-11-17 |
| lcri02hcq | 13972 | HIP66578 | TT | EXT/SCI | 181 | P2 | Low | BOA | MIRB | 22.1 | -153.1 | 2015-10-06 |
| lcri02hgq | 13972 | HIP66578 | ACCUM | ACQ/IMAGE | 181 | P2 | Med | BOA | MIRB | 22.1 | -153.1 | 2015-10-06 |
| ld3702n4q | 14440 | HIP66578 | TT | EXT/SCI | 183 | P2 | Low | BOA | MIRB | 22.1 | -153.1 | 2016-10-19 |
| ld3702n9q | 14440 | HIP66578 | ACCUM | ACQ/IMAGE | 183 | P2 | Med | BOA | MIRB | 22.1 | -153.1 | 2016-10-19 |
| ldozbbliq | 14857 | HIP66578 | TT | EXT/SCI | 183 | P2 | Low | BOA | MIRB | 22.1 | -153.1 | 2017-09-06 |
| ldozbblmq | 14857 | HIP66578 | ACCUM | ACQ/IMAGE | 183 | P2 | Med | BOA | MIRB | 22.1 | -153.1 | 2017-09-06 |

[c] The P2 wavelength calibration lamp current settings are LOW (3 mA), MED (10 mA) and HIGH (14 mA).

[t] TT = TIME-TAG.

[x] *APERYPOS*, the AD aperture mechanism positions, are stored in the FSW in PCMECH_APMDISPPOSITION. The trailing "0.1" reported in the FITS headers is a conversion anomaly that is present in all aperture positions (*APERXPOS* & *APERYPOS*).

[y] It is not uncommon that the XD aperture location (*APERXPOS*) is ± one step off from its nominal position. The XD aperture mechanism positions are stored in the FSW in PCMECH_APMXDISPPOSITION (see Table **??**).

Note. — PSA EXPTYPE=EXT/SCI exposures contain coeval target and PtNe lamp TT images.

Table 4. COS/NUV TA Monitoring Imaging Exposures - WCA only

| *ROOTNAME* | *PROPOSID* | *TARGNAME* | *OBSMODE*[t] | *EXPTYPE* | *EXPTIME* (s) | PtNe Lamp # | Lamp Current[c] | *APERTURE* | *OPT_ELEM* | *APERXPOS*[x] | *APERYPOS*[y] | *DATE-OBS* |
|---|---|---|---|---|---|---|---|---|---|---|---|---|
| (1) | (2) | (3) | (4) | (5) | (6) | (7) | (8) | (9) | (10) | (11) | (12) | (13) |
| | | | | | WCA × MIRA | | | | | | | |
| lcgp01byq | 13523 | WAVE | TT | WAVECAL | 20 | P2 | Low | WCA | MIRA | 22.1 | 127.1 | 2013-11-11 |
| lcgp01c3q | 13523 | WAVE | TT | WAVECAL | 20 | P1 | Low | WCA | MIRA | 22.1 | 127.1 | 2013-11-11 |
| lcgq01qbq | 13526 | WAVE | TT | WAVECAL | 7 | P2 | Low | WCA | MIRA | 22.1 | 126.1 | 2014-11-19 |
| lcgq01qfq | 13526 | WAVE | TT | WAVECAL | 7 | P2 | Low | WCA | MIRA | 22.1 | 126.1 | 2014-11-19 |
| lcgq02hoq | 13526 | WAVE | TT | WAVECAL | 7 | P2 | Low | WCA | MIRA | 22.1 | 126.1 | 2014-11-17 |
| lcgq02hyq | 13526 | WAVE | TT | WAVECAL | 10 | P2 | Low | WCA | MIRA | 22.1 | 126.1 | 2014-11-17 |
| lcgq02icq | 13526 | WAVE | TT | WAVECAL | 10 | P1 | Low | WCA | MIRA | 22.1 | 127.1 | 2014-11-17 |
| lcgq02ieq | 13526 | WAVE | TT | WAVECAL | 10 | P2 | Low | WCA | MIRA | 22.1 | 127.1 | 2014-11-17 |
| lcri01g5q | 13972 | WAVE | TT | WAVECAL | 10 | P2 | Low | WCA | MIRA | 22.1 | 126.1 | 2015-10-06 |
| lcri01g9q | 13972 | WAVE | TT | WAVECAL | 10 | P2 | Low | WCA | MIRA | 22.1 | 126.1 | 2015-10-06 |
| lcri02haq | 13972 | WAVE | TT | WAVECAL | 14 | P2 | Low | WCA | MIRA | 22.1 | 126.1 | 2015-10-06 |
| lcri02hkq | 13972 | WAVE | TT | WAVECAL | 14 | P2 | Low | WCA | MIRA | 22.1 | 126.1 | 2015-10-06 |
| lcri02hyq | 13972 | WAVE | TT | WAVECAL | 14 | P1 | Low | WCA | MIRA | 22.1 | 125.1 | 2015-10-06 |
| lcri02i0q | 13972 | WAVE | TT | WAVECAL | 24 | P2 | Low | WCA | MIRA | 22.1 | 125.1 | 2015-10-06 |
| ld3701gzq | 14440 | WAVE | TT | WAVECAL | 9 | P2 | Low | WCA | MIRA | 22.1 | 126.1 | 2016-10-18 |
| ld3701h3q | 14440 | WAVE | TT | WAVECAL | 10 | P2 | Low | WCA | MIRA | 22.1 | 126.1 | 2016-10-18 |
| ld3702n1q | 14440 | WAVE | TT | WAVECAL | 14 | P2 | Low | WCA | MIRA | 22.1 | 126.1 | 2016-10-19 |
| ld3702neq | 14440 | WAVE | TT | WAVECAL | 14 | P2 | Low | WCA | MIRA | 22.1 | 126.1 | 2016-10-19 |
| ld3702o1q | 14440 | WAVE | TT | WAVECAL | 14 | P1 | Low | WCA | MIRA | 22.1 | 125.1 | 2016-10-19 |
| ld3702o3q | 14440 | WAVE | TT | WAVECAL | 24 | P2 | Low | WCA | MIRA | 22.1 | 125.1 | 2016-10-19 |
| ldozbadnq | 14857 | WAVE | TT | WAVECAL | 9 | P2 | Low | WCA | MIRA | 22.1 | 126.1 | 2017-09-04 |
| ldozbadrq | 14857 | WAVE | TT | WAVECAL | 10 | P2 | Low | WCA | MIRA | 22.1 | 126.1 | 2017-09-04 |
| ldozbblgq | 14857 | WAVE | TT | WAVECAL | 14 | P2 | Low | WCA | MIRA | 22.1 | 126.1 | 2017-09-06 |
| ldozbblqq | 14857 | WAVE | TT | WAVECAL | 14 | P2 | Low | WCA | MIRA | 22.1 | 126.1 | 2017-09-06 |
| ldozbbm4q | 14857 | WAVE | TT | WAVECAL | 16 | P1 | Low | WCA | MIRA | 22.1 | 125.1 | 2017-09-06 |
| ldozbbm6q | 14857 | WAVE | TT | WAVECAL | 26 | P2 | Low | WCA | MIRA | 22.1 | 125.1 | 2017-09-06 |
| | | | | | WCA × MIRB | | | | | | | |
| lcgp01bpq | 13523 | WAVE | TT | WAVECAL | 40 | P2 | Low | WCA | MIRB | 22.1 | 127.1 | 2013-11-11 |
| lcgp01bsq | 13523 | WAVE | TT | WAVECAL | 40 | P1 | Low | WCA | MIRB | 22.1 | 127.1 | 2013-11-11 |
| lcgq02hsq | 13526 | WAVE | TT | WAVECAL | 12 | P2 | Med | WCA | MIRB | 22.1 | 126.1 | 2014-11-17 |
| lcgq02hwq | 13526 | WAVE | TT | WAVECAL | 12 | P2 | Med | WCA | MIRB | 22.1 | 126.1 | 2014-11-17 |
| lcgq02igq | 13526 | WAVE | TT | WAVECAL | 30 | P1 | Low | WCA | MIRB | 22.1 | 127.1 | 2014-11-17 |
| lcgq02iiq | 13526 | WAVE | TT | WAVECAL | 20 | P2 | Med | WCA | MIRB | 22.1 | 127.1 | 2014-11-17 |
| lcri02heq | 13972 | WAVE | TT | WAVECAL | 24 | P2 | Med | WCA | MIRB | 22.1 | 126.1 | 2015-10-06 |
| lcri02hiq | 13972 | WAVE | TT | WAVECAL | 24 | P2 | Med | WCA | MIRB | 22.1 | 126.1 | 2015-10-06 |
| lcri02i2q | 13972 | WAVE | TT | WAVECAL | 30 | P1 | Low | WCA | MIRB | 22.1 | 125.1 | 2015-10-06 |
| lcri02i4q | 13972 | WAVE | TT | WAVECAL | 24 | P2 | Med | WCA | MIRB | 22.1 | 125.1 | 2015-10-06 |
| ld3702n7q | 14440 | WAVE | TT | WAVECAL | 24 | P2 | Med | WCA | MIRB | 22.1 | 126.1 | 2016-10-19 |
| ld3702nbq | 14440 | WAVE | TT | WAVECAL | 24 | P2 | Med | WCA | MIRB | 22.1 | 126.1 | 2016-10-19 |
| ld3702o5q | 14440 | WAVE | TT | WAVECAL | 30 | P1 | Low | WCA | MIRB | 22.1 | 125.1 | 2016-10-19 |
| ld3702o7q | 14440 | WAVE | TT | WAVECAL | 24 | P2 | Med | WCA | MIRB | 22.1 | 125.1 | 2016-10-19 |
| ldozbblkq | 14857 | WAVE | TT | WAVECAL | 24 | P2 | Med | WCA | MIRB | 22.1 | 126.1 | 2017-09-06 |
| ldozbbloq | 14857 | WAVE | TT | WAVECAL | 24 | P2 | Med | WCA | MIRB | 22.1 | 126.1 | 2017-09-06 |
| ldozbbm8q | 14857 | WAVE | TT | WAVECAL | 32 | P1 | Low | WCA | MIRB | 22.1 | 125.1 | 2017-09-06 |
| ldozbbmaq | 14857 | WAVE | TT | WAVECAL | 26 | P2 | Med | WCA | MIRB | 22.1 | 125.1 | 2017-09-06 |

[c] The P2 wavelength calibration lamp current settings are LOW (6mA), MED (10mA) and HIGH (18mA). The P2 wavelength calibration lamp current settings are LOW (3mA), MED (10mA) and HIGH (14mA).

[t] TT = TIME-TAG.

[x] *APERYPOS*, the AD aperture mechanism positions are stored in the FSW in PCMECH_APMDISPPOSITION. The trailing "0.1" reported in the FITS headers is a conversion anomaly that is present in all aperture positions (*APERXPOS* & *APERYPOS*).

[y] It is not uncommon that the XD aperture location (*APERXPOS*) is ± one step off from its nominal position.

Note. — All exposures in this table are *EXPTYPE*=WAVECAL (target = WAVE) and contain only TT PtNe lamp (WCA) images, and the indicated MIRROR position (*OPT_ELEM*).

Table 5. NUV Spectroscopic TA Monitoring Exposures

| *ROOTNAME* | *PROPOSID* | *TARGNAME* | *EXPTIME* (s) | *OPT_ELEM* | *CENWAVE* | LP *LIFE_ADJ* | *APERXPOS* | *APERYPOS*[a] | *DATE-OBS* |
|---|---|---|---|---|---|---|---|---|---|
| (1) | (2) | (3) | (4) | (5) | (6) | (7) | (8) | (9) | (10) |
| lcgq01qlq | 13526 | WD-1657+343 | 20 | G230L | 3000 | 1 | 22.1 | 126.1 | 2014-11-19 |
| lcgq01r6q | 13526 | WD-1657+343 | 151 | G285M | 2850 | 1 | 22.1 | 126.1 | 2014-11-19 |
| lcgq02i2q | 13526 | HIP66578 | 40 | G185M | 1890 | 1 | 22.1 | 126.1 | 2014-11-17 |
| lcgq02i4q | 13526 | HIP66578 | 52 | G225M | 2306 | 1 | 22.1 | 126.1 | 2014-11-17 |
| lcri01ggq | 13972 | WD-1657+343 | 20 | G230L | 3000 | 1 | 22.1 | 126.1 | 2015-10-06 |
| lcri01giq | 13972 | WD-1657+343 | 151 | G285M | 2676 | 1 | 22.1 | 126.1 | 2015-10-06 |
| lcri02hoq | 13972 | HIP66578 | 52 | G225M | 2306 | 1 | 22.1 | 126.1 | 2015-10-06 |
| lcri02hqq | 13972 | HIP66578 | 40 | G185M | 1913 | 1 | 22.1 | 126.1 | 2015-10-06 |
| ld3701h9q | 14440 | WD-1657+343 | 21 | G230L | 3000 | 1 | 22.1 | 126.1 | 2016-10-18 |
| ld3701hbq | 14440 | WD-1657+343 | 151 | G285M | 2676 | 1 | 22.1 | 126.1 | 2016-10-18 |
| ld3702nmq | 14440 | HIP66578 | 53 | G225M | 2306 | 1 | 22.1 | 126.1 | 2016-10-19 |
| ld3702noq | 14440 | HIP66578 | 40 | G185M | 1913 | 1 | 22.1 | 126.1 | 2016-10-19 |
| ldozbadxq | 14857 | WD-1657+343 | 23 | G230L | 3000 | 1 | 22.1 | 126.1 | 2017-09-04 |
| ldozbadzq | 14857 | WD-1657+343 | 151 | G285M | 2676 | 1 | 22.1 | 126.1 | 2017-09-04 |
| ldozbbluq | 14857 | HIP66578 | 53 | G225M | 2306 | 1 | 22.1 | 126.1 | 2017-09-06 |
| ldozbblwq | 14857 | HIP66578 | 40 | G185M | 1913 | 1 | 22.1 | 126.1 | 2017-09-06 |

[a]The NUV (LP1) XD location of the aperture (*APERYPOS*) is 126 in the FSW table `pcmech_ApMXDispPosition`.).

Note. — All exposures were taken with the PSA at `FP-POS=3`. All exposures executed at the expected aperture position (*APERXPOS* & *APERYPOS*).

Table 6. FUV TA Monitoring Exposures

| *ROOTNAME* (1) | *PROPOSID* (2) | *TARGNAME* (3) | *EXPTIME* (s) (4) | *OPT_ELEM* (5) | *CENWAVE* (6) | LP (7) | *APERXPOS* (8) | *APERYPOS* (9) | *DATE-OBS* (10) |
|---|---|---|---|---|---|---|---|---|---|
| lcgq01r8q | 13526 | WD-1657+343 | 20 | G130M | 1309 | 2 | 22.1 | 52.1 | 2014-11-19 |
| lcgq01r8q | 13526 | WD-1657+343 | 20 | G130M | 1309 | 2 | 22.1 | 52.1 | 2014-11-19 |
| lcgq01raq | 13526 | WD-1657+343 | 7 | G140L | 1280 | 2 | 22.1 | 52.1 | 2014-11-19 |
| lcgq01raq | 13526 | WD-1657+343 | 7 | G140L | 1280 | 2 | 22.1 | 52.1 | 2014-11-19 |
| lcgq02i6q | 13526 | HIP66578 | 18 | G160M | 1600 | 2 | 22.1 | 52.1 | 2014-11-17 |
| lcgq02i8q | 13526 | HIP66578 | 22 | G160M | 1600 | 2 | 22.1 | 52.1 | 2014-11-17 |
| lcgq02iaq | 13526 | HIP66578 | 22 | G160M | 1600 | 2 | 22.1 | 52.1 | 2014-11-17 |
| lcri01gkq | 13972 | WD-1657+343 | 20 | G130M | 1309 | 3 | 22.1 | 182.1 | 2015-10-06 |
| lcri01gkq | 13972 | WD-1657+343 | 20 | G130M | 1309 | 3 | 22.1 | 182.1 | 2015-10-06 |
| lcri01h6q | 13972 | WD-1657+343 | 7 | G140L | 1280 | 3 | 22.1 | 182.1 | 2015-10-06 |
| lcri01h6q | 13972 | WD-1657+343 | 7 | G140L | 1280 | 3 | 22.1 | 182.1 | 2015-10-06 |
| lcri02hsq | 13972 | HIP66578 | 22 | G160M | 1600 | 3 | 22.1 | 182.1 | 2015-10-06 |
| lcri02huq | 13972 | HIP66578 | 25 | G160M | 1600 | 3 | 22.1 | 182.1 | 2015-10-06 |
| lcri02hwq | 13972 | HIP66578 | 25 | G160M | 1600 | 3 | 22.1 | 182.1 | 2015-10-06 |
| ld3701hdq | 14440 | WD-1657+343 | 25 | G130M | 1309 | 3 | 22.1 | 182.1 | 2016-10-18 |
| ld3701hdq | 14440 | WD-1657+343 | 25 | G130M | 1309 | 3 | 22.1 | 182.1 | 2016-10-18 |
| ld3701hfq | 14440 | WD-1657+343 | 10 | G140L | 1280 | 3 | 22.1 | 182.1 | 2016-10-18 |
| ld3701hfq | 14440 | WD-1657+343 | 10 | G140L | 1280 | 3 | 22.1 | 182.1 | 2016-10-18 |
| ld3702nqq | 14440 | HIP66578 | 22 | G160M | 1600 | 3 | 22.1 | 182.1 | 2016-10-19 |
| ld3702nsq | 14440 | HIP66578 | 25 | G160M | 1600 | 3 | 22.1 | 182.1 | 2016-10-19 |
| ld3702nuq | 14440 | HIP66578 | 25 | G160M | 1600 | 3 | 22.1 | 182.1 | 2016-10-19 |
| ldozbae1q | 14857 | WD-1657+343 | 25 | G130M | 1309 | 3 | 22.1 | 182.1 | 2017-09-04 |
| ldozbae1q | 14857 | WD-1657+343 | 25 | G130M | 1309 | 3 | 22.1 | 182.1 | 2017-09-04 |
| ldozbae3q | 14857 | WD-1657+343 | 10 | G140L | 1280 | 3 | 22.1 | 182.1 | 2017-09-04 |
| ldozbae3q | 14857 | WD-1657+343 | 10 | G140L | 1280 | 3 | 22.1 | 182.1 | 2017-09-04 |
| ldozbblyq | 14857 | HIP66578 | 22 | G160M | 1600 | 3 | 22.1 | 182.1 | 2017-09-06 |
| ldozbbm0q | 14857 | HIP66578 | 27 | G160M | 1600 | 3 | 22.1 | 182.1 | 2017-09-06 |
| ldozbbm2q | 14857 | HIP66578 | 27 | G160M | 1600 | 3 | 22.1 | 182.1 | 2017-09-06 |

Note. — All exposures were taken with the PSA at *FP-POS=3*. All exposures executed at the expected aperture positions (*APERXPOS* & *APERYPOS*).

# 4 Verifying the TA (ACQ/) Subarrays

COS TA subarrays are loaded during the HST ground commanding uniquely for each TA exposure, and are ACQ/ mode, NUV stripe (*STRIPE*), *CENWAVE* , and FUV segment *SEGMENT* and LP dependent. Additionally, these subarrays change with time in response to detector (e.g., increasing background or "hot-spots) or mechanism (e.g., secular OSM drift) monitoring. There are two stages to the TA verification, 1) ensuring that the intended subarrays were commanded as intended, and 2) that those subarrays were valid for the entire duration of usage.

Ideally, one would compare that commanded subarrays for all exposures to those reported in the _rawacq.fits. However, due to issues with the COS TA subarrays[29], in this ISR, the subarrays were inferred from the telemetry reported in the _spt.fits files.

Tables **??**, **??**, **??**, **??** give the TA subarrays for all imaging modes as it has evolved since SMOV. Table **??** gives the TA subarrays for all NUV spectroscopic ACQ/SEARCH and ACQ/PEAKKD that have executed use since SMOV, and Table **??** gives the TA subarrays for all NUV ACQ/PEAKXDs since SMOV. Table **??** gives the TA subarrays for the WCA portion of all FUV ACQ/PEAKXDs separated by LP and *CENWAVE* . Table **??** gives the TA subarrays for the WCA portion of all FUV ACQ/PEAKXDs separated by LP and *CENWAVE* .

Table **??** gives the TA subarrays for the PSA/BOA portion of all FUVA ACQ/s separated by LP and *CENWAVE* , and Table **??** gives the TA subarrays for all LPs and *CENWAVE*s for FUVB. Note that TA has not been enabled for all FUV *CENWAVE*s , so only the TA subarrays that are in use are listed. The FUV table includes subarrays for all four COS LPs even though only the LP2 and LP3 subarrays were monitored in this ISR.

All values indicate that the intended subarrays are being used for all TA and science exposures. All FUV spectra were visually inspected to verify that the TA subarrays were successfully excluding all known detector hot-spots and the bright Geocoronal emission lines that can negatively affect TAs. No action is required based upon this analysis of the TA and science subarrays used in C21.

COS TA subarrays are defined in detector coordinates, and are specified by giving the [X,Y] corners ([XC,YC]) and sizes ([XS,YS]). Table **??** below gives the NUV spectroscopic TA subarrays used for ACQ/SEARCH and ACQ/PEAKD, which have not changed since SMOV. Table **??** below gives the NUV spectroscopic TA subarrays used for ACQ/PEAKXD, which include subarrays to measure the calibration lamp XD location (WCA) as well as the target spectral location of *STRIPE=B (MEDIUM)*). These have not changed there updated in 2010 as *PR#*XXX.

In this section, we describe the various subarrays used in COS TA. These subarrays are defined by giving the detector coordinate of the lowest valued corner (C) and the full size (S) for both X and Y. A subarray is fully specified by giving its XC, XS, YC, and YS. Unless noted, coordinates are in detector coordinates as this is the system in which COS TAs are performed.

TA subarrays are necessary to remove unwanted detector background or spectral or detector features not associated with the target, such as detector "hot-spots" or Geocoronal emission (see Penton & Keyes, 2011). All COS ACQ/ modes use subarrays, but they different for each mode, detector or detector segment, and *CENWAVE* . The explanation for the sizes and locations of the TA subarrays are beyond the scope of this ISR, but can be found in the TIR COS-2010-03 (Penton & Keyes, 2011), the pre-launch estimates (driven by ray-trace predictions; COS-11-0024A (Penton, 2001), COS-11-0014B (Penton, 2002), & COS-11-0016A (Penton, 2001) and for FUV LP2–4 in

[29] This issues should be addressed for C26 with the corrections outlined in *PR#*64849, *PR#*64874, & *PR#*66840

Table 7. 2009–2011.016 ACQ/IMAGE and ACQ/SEARCH Subarrays.

| Aperture | MIRROR | XC | YC | XS | YS |
|---|---|---|---|---|---|
| WCA | MIRA | 268 | 95 | 200 | 660 |
| WCA | MIRB | 103 | 361 | 200 | 660 |
| PSA/BOA | MIRA | 572 | 108 | 345 | 816 |
| PSA/BOA | MIRB | 410 | 200 | 345 | 816 |

Note. — Due to increased detector background, these were updated on 2011.017 (*PR#*67139) as described in Penton & Keyes (2011).

their respective enabling ISRs (Penton 2018 (LP2), Penton 2018 (LP3) and Penton & White 2018 (LP4).) The programs discussed in this ISR do not contain any FUV or NUV spectroscopic ACQ/ exposures, therefore, the bulk of the discussion for the TA subarrays for spectroscopic TAs are contained in the respective enabling ISRs. The spectroscopic exposures discussed in this ISR will, however, be used to verify the appropriateness of the XD locations of the subarrays in § **??** (NUV) and § **??**.

## 4.1 NUV Imaging TA subarrays

The original (2009) NUV imaging ACQ/IMAGE and ACQ/SEARCH TA subarrays are given in Table **??**. This table includes entries for the WCA and PSA and both MIRA and MIRB. The COS FSW uses the same subarrays for the PSA and BOA as the offset on the detector between the aperture locationss is small ($\Delta$ [AD,XD]$\sim$[11.0,0.4]p).

Due to rising NUV detector background, and supported by an analysis of OSM repeatability, reductions to the PSA/BOA ACQ/SEARCH and WCA ACQ/IMAGE subarrays sizes were implemented on 2011.017 (STScI *PR#*67139)[30]. During ACQ/IMAGE, the region of the detector used to determine the source location is small, and is given by the square of the TA parameter PCTA_CHECKBOXSIZE, which is currently set to 9p (81 total pixels). There no adjustment was warranted for the PSA/BOA ACQ/IMAGE subarrays. However, during ACQ/SEARCH, the counts in the full subarray are used (currently $345 \times 816$=19,376p). NUV ACQ/SEARCH TAs are therefore much more vulnerable (by a factor of 3500) to contamination from background events and SAA passages (Penton & Keyes, 2011). The updated ACQ/SEARCH values are given in Table **??**, and the updated ACQ/IMAGE subarrays are given in Table **??**.

[30]On-orbit analysis of the OSM positions showed that the the WCA LTAIMCAL MIRA and MIRB lamp image detector locatians were fairly repeatable (usually with $\pm$ 50 AD p and $\pm$ 10 XDp). As discussed in Penton & Keyes (2011), the WCA TA ACQ/IMAGE subarrays were reduced by $\pm$ 50p in XD and $\pm$ 180p in AD, and ACQ/SEARCH subarrays were reduced by 125 AD p and 346 XD p.

Table 8. 2011.017–2014.299 `ACQ/IMAGE` Subarrays.

| Aperture | MIRROR | XC | YC | XS | YS |
|---|---|---|---|---|---|
| WCA | MIRA | **345** | **324** | **50** | **300** |
| WCA | MIRB | **184** | **539** | **50** | **300** |
| PSA/BOA | MIRA | 572 | 108 | 345 | 816 |
| PSA/BOA | MIRB | 410 | 200 | 345 | 816 |

Note. — **Bold** values in this table were updated on 2011.017 (*PR#*67139) due to increased detector background, as described in Penton & Keyes (2011).

Table 9. 2011.017–Present COS `ACQ/SEARCH` TA Subarrays.

| *APERTURE* | MIRROR | XC | YC | XS | YS |
|---|---|---|---|---|---|
| PSA/BOA | MIRA | 630 | 284 | 220 | 470 |
| PSA/BOA | MIRB | 469 | 499 | 220 | 470 |

Note. — Updated on 2011.017 (*PR#*67139), as described in Penton & Keyes (2011).

Table 10. 2014.300–Present ACQ/IMAGE Subarrays.

| *APERTURE* | MIRROR | XC | YC | XS | YS |
|---|---|---|---|---|---|
| WCA | MIRA | 345 | 324 | 50 | 300 |
| WCA | MIRB | **187** | **566** | 50 | 300 |
| PSA/BOA | MIRA | 572 | 108 | 345 | 816 |
| PSA/BOA | MIRB | 410 | 200 | 345 | 816 |

Note. — Due to errors in determining the WCA AD position due to increased NUV detector background, the **bold** subarrays values were updated on Oct. 6, 2014 (2014.279) with *PR#*78749. Simultaneously, the MIRB ACQ/ lamp exposure time and current settings (for the P2 lamp) were changed from 17s @ LOW current to 12s @ MED current (*PR#*78749). The FSW WCA-to-SA offsets ([X,Y]IMCALTARGETOFFSET) were adjusted accordingly (*PR#*79116) on October 16, 2014 (2014.289), prior to use by HST users on Nov. 10, 2014 (2014.314). The default exposure time and current for the P1 lamp image “TAGFLASH”s were changed later with *PR#*84463.

## 4.2 COS NUV Spectroscopic TA Subarrays

The NUV spectroscopic TA subarrays for the ACQ/SEARCH and ACQ/PEAKD phases are identical, and are given in Table **??**. These subarrays are not grating-specific and are large enough to capture the flux from all three stripes (two for G230L; *STRIPE=C (LONG)* is not used for G230L TA). COS uses the same NUV TA subarrays for the PSA and BOA as the XD offset between the NUV spectra is small ($\Delta$XD$\sim$5p).

The NUV spectroscopic TA SA subarrays for the ACQ/PEAKXD are given in Table **??**. These subarrays are large enough to only capture the flux from a single NUV stripe. Stripe-specific subarrays are defined for both the WCA and PSA. If used with an extended source, these subarrays are vulnerable to cross-contamination of stripe light. In this table, only the values of XC are listed. For all NUV ACQ/PEAKXDs, YC=0, YS=1024, and XS=81.

## 4.3 COS FUV Spectroscopic TA Subarrays

The FUV spectroscopic TA subarrays for the WCA are the same for ACQ/SEARCH, ACQ/PEAKD, and ACQ/PEAKXD and are given in Table **??** for both FUVA and FUVB. Only one subarray is used for the WCA for each FUV segment, these are labeled ‘A1’ and ‘B1’. As the data are taken in “detector” coordinates, all FUV TA subarrays values are valid only for the normal operating temperature range of COS. FUVB is not used in G140L TAs.

The FUV spectroscopic subarrays used for all external targets at LP1–4 for FUVA are given in Table **??** and for FUVB in Table **??**. There are two subarrays used for each FUV segment, these are

Table 11. FITS Reported TA ACQ/IMAGE Subarrays

| *PROPOSID* (PID) | IPPPSSOOT | *APERTURE* ×MIRROR | WCA XC | WCA YC | WCA XS | WCA YS | SA (PSA or BOA) XC | SA YC | SA XS | SA YS | *DATE-OBS* |
|---|---|---|---|---|---|---|---|---|---|---|---|
| MIRA ACQ/IMAGE Subarrays | | | | | | | | | | | |
| 13171 | lc6ka1i1q | PSA×MIRA | 345 | 324 | 50 | 300 | 572 | 108 | 345 | 816 | 2013-03-02 |
| 13171 | lc6ka2imq | PSA×MIRA | 345 | 324 | 50 | 300 | 572 | 108 | 345 | 816 | 2013-09-01 |
| 13616 | lci4a1dcq | PSA×MIRA | 345 | 324 | 50 | 300 | 572 | 108 | 345 | 816 | 2014-04-03 |
| 13616 | lci4a2e3q | PSA×MIRA | 345 | 324 | 50 | 300 | 572 | 108 | 345 | 816 | 2014-10-27 |
| 13526 | lcgq01qdq | BOA×MIRA | 345 | 324 | 50 | 300 | 572 | 108 | 345 | 816 | 2014-11-19 |
| 13526 | lcgq02hmq | BOA×MIRA | 345 | 324 | 50 | 300 | 572 | 108 | 345 | 816 | 2014-11-17 |
| 13526 | lcgq02i0q | BOA×MIRA | 345 | 324 | 50 | 300 | 572 | 108 | 345 | 816 | 2014-11-17 |
| 13526 | lcgq03dbq | PSA×MIRA | 345 | 324 | 50 | 300 | 572 | 108 | 345 | 816 | 2014-10-06 |
| 13526 | lcgq03dtq | PSA×MIRA | 345 | 324 | 50 | 300 | 572 | 108 | 345 | 816 | 2014-10-06 |
| 14035 | lcsla1i4q | PSA×MIRA | 345 | 324 | 50 | 300 | 572 | 108 | 345 | 816 | 2015-04-14 |
| 14035 | lcsla2bhq | PSA×MIRA | 345 | 324 | 50 | 300 | 572 | 108 | 345 | 816 | 2015-10-02 |
| 13972 | lcri01g7q | BOA×MIRA | 345 | 324 | 50 | 300 | 572 | 108 | 345 | 816 | 2015-10-06 |
| 13972 | lcri02h8q | BOA×MIRA | 345 | 324 | 50 | 300 | 572 | 108 | 345 | 816 | 2015-10-06 |
| 13972 | lcri02hmq | BOA×MIRA | 345 | 324 | 50 | 300 | 572 | 108 | 345 | 816 | 2015-10-06 |
| 14440 | ld3701h1q | BOA×MIRA | 345 | 324 | 50 | 300 | 572 | 108 | 345 | 816 | 2016-10-18 |
| 14440 | ld3702mzq | BOA×MIRA | 345 | 324 | 50 | 300 | 572 | 108 | 345 | 816 | 2016-10-19 |
| 14440 | ld3702nhq | BOA×MIRA | 345 | 324 | 50 | 300 | 572 | 108 | 345 | 816 | 2016-10-19 |
| 14857 | ldozbadpq | BOA×MIRA | 345 | 324 | 50 | 300 | 572 | 108 | 345 | 816 | 2017-09-04 |
| 14857 | ldozbbleq | BOA×MIRA | 345 | 324 | 50 | 300 | 572 | 108 | 345 | 816 | 2017-09-06 |
| 14857 | ldozbblsq | BOA×MIRA | 345 | 324 | 50 | 300 | 572 | 108 | 345 | 816 | 2017-09-06 |
| 14857 | ldozpbf5q | PSA×MIRA | 345 | 324 | 50 | 300 | 572 | 108 | 345 | 816 | 2017-09-10 |
| 14857 | ldozpbfhq | PSA×MIRA | 345 | 324 | 50 | 300 | 572 | 108 | 345 | 816 | 2017-09-10 |
| MIRB ACQ/IMAGE Subarrays | | | | | | | | | | | |
| 13171 | lc6ka1i3q | PSA×MIRB | 184 | 539 | 50 | 300 | 411 | 200 | 345 | 816 | 2013-03-02 |
| 13171 | lc6ka1i3q | PSA×MIRB | 184 | 539 | 50 | 300 | 411 | 200 | 345 | 816 | 2013-03-02 |
| 13171 | lc6ka2ioq | PSA×MIRB | 184 | 539 | 50 | 300 | 411 | 200 | 345 | 816 | 2013-09-01 |
| 13171 | lc6ka2ioq | PSA×MIRB | 184 | 539 | 50 | 300 | 411 | 200 | 345 | 816 | 2013-09-01 |
| 13616 | lci4a1deq | PSA×MIRB | 184 | 539 | 50 | 300 | 411 | 200 | 345 | 816 | 2014-04-03 |
| 13616 | lci4a2e5q | PSA×MIRB | 187 | 566 | 50 | 300 | 411 | 200 | 345 | 816 | 2014-10-27 |
| 13526 | lcgq01q5q | PSA×MIRB | 187 | 566 | 50 | 300 | 411 | 200 | 345 | 816 | 2014-11-19 |
| 13526 | lcgq01qjq | PSA×MIRB | 187 | 566 | 50 | 300 | 411 | 200 | 345 | 816 | 2014-11-19 |
| 13526 | lcgq02huq | BOA×MIRB | 187 | 566 | 50 | 300 | 411 | 200 | 345 | 816 | 2014-11-17 |
| 13526 | lcgq03dlq | PSA×MIRB | 187 | 566 | 50 | 300 | 411 | 200 | 345 | 816 | 2014-10-06 |
| 13972 | lcri01fzq | PSA×MIRB | 187 | 566 | 50 | 300 | 411 | 200 | 345 | 816 | 2015-10-06 |
| 13972 | lcri01geq | PSA×MIRB | 187 | 566 | 50 | 300 | 411 | 200 | 345 | 816 | 2015-10-06 |
| 13972 | lcri02hgq | BOA×MIRB | 187 | 566 | 50 | 300 | 411 | 200 | 345 | 816 | 2015-10-06 |
| 14035 | lcsla1i6q | PSA×MIRB | 187 | 566 | 50 | 300 | 411 | 200 | 345 | 816 | 2015-04-14 |
| 14035 | lcsla2bjq | PSA×MIRB | 187 | 566 | 50 | 300 | 411 | 200 | 345 | 816 | 2015-10-02 |
| 14440 | ld3701gtq | PSA×MIRB | 187 | 566 | 50 | 300 | 411 | 200 | 345 | 816 | 2016-10-18 |
| 14440 | ld3701h7q | PSA×MIRB | 187 | 566 | 50 | 300 | 411 | 200 | 345 | 816 | 2016-10-18 |
| 14440 | ld3702n9q | BOA×MIRB | 187 | 566 | 50 | 300 | 411 | 200 | 345 | 816 | 2016-10-19 |
| 14857 | ldozbadhq | PSA×MIRB | 187 | 566 | 50 | 300 | 411 | 200 | 345 | 816 | 2017-09-04 |
| 14857 | ldozbadvq | PSA×MIRB | 187 | 566 | 50 | 300 | 411 | 200 | 345 | 816 | 2017-09-04 |
| 14857 | ldozbblmq | BOA×MIRB | 187 | 566 | 50 | 300 | 411 | 200 | 345 | 816 | 2017-09-06 |
| 14857 | ldozpbfbq | PSA×MIRB | 187 | 566 | 50 | 300 | 411 | 200 | 345 | 816 | 2017-09-10 |

Note. — As correctly reported in the FITS files, the MIRB subarrays values were updated from [XC,YC]=[184,539] to [187,566] on Oct. 6, 2014 (2014.279) with *PR#*78749. Simultaneously, the MIRB ACQ/ lamp exposure time and current settings (for the P2 lamp) TAsubarrays.tex:were changed from 17s @ LOW current to 12s @ MED current (*PR#*78749). The FSW WCA-to-SA offsets ([X,Y]IMCALTARGETOFFSET) were adjusted accordingly (*PR#*79116) on October 16, 2014 (2014.289)

Table 12 NUV Spectroscopic ACQ/SEARCH and ACQ/PEAKD Sub-arrays

| *OPT_ELEM* | XC | YC | XS | YS |
|---|---|---|---|---|
| G185M | 509 | 0 | 420 | 1024 |
| G225M | 512 | 0 | 420 | 1024 |
| G285M | 499 | 0 | 420 | 1024 |
| G230L | 659 | 0 | 275 | 1024 |

[1] NUV ACQ/SEARCH and ACQ/PEAKD external target (SA) subarrays. NUV ACQ/PEAKXD lamp and SA subarrays are given in **??**.
[2] Installed by HST commanding on 2009.201 (*PR#*63095).

Table 13 NUV ACQ/PEAKXD Subarray "XC"s[1]

| *OPT_ELEM* | WCA-A | WCA-B | WCA-C | SCI-A | SCI-B | SCI-C |
|---|---|---|---|---|---|---|
| G185M | 418 | 327 | 192 | 794 | 700 | 565 |
| G225M | 430 | 327 | 186 | 804 | 703 | 560 |
| G285M | 407 | 313 | 180 | 782 | 688 | 555 |
| G230L | 433 | 334 | 194 | 807 | 707 | 564 |

[1] XC = X-Corner. For all NUV ACQ/PEAKXD TA subarrays: YC=0, YS=1024, and XS=81; where S=Size. Updated on July 19, 2009 (2009.200) with *PR#*63095. Some early calibration observations used slightly different values.

labeled 'A1', 'A2', 'B1', and 'B2'. The COS FSW uses the same subarrays for the PSA and BOA as the offset between the FUV spectra is small ($\Delta$ XD$\sim$3p). As with the other HST spectrographs, FUV TAs are susceptible to contamination from geocoronal light , particularly Ly$\alpha$ 1216Å, OI 1302Å, and SiII1304Å (Penton & Keyes, 2010). The FUV TA subarrays outlined in tables **??** and **??** have been tailored to remove regions of the target spectrum that may contain Geocoronal light. The Geocoronal light fills the aperture and has a very different XD profile which could cause problems with FUV TAs.

In 2014–5, several "hot-spots" appeared during solar maximum. On April 20, 2015 (2015.110) with *PR#*80571, the FUV LP3 subarrays were adjusted to avoid these hot-spots. Details are given in § **??**, and the adjusted FUVB subarrays are also given in Table **??**.

## 4.4 Trimming of COS FUV TA subarrays due to FUVB "Hot-Spot".

A "hot-spot" appeared on the COS FUVB segment coincident with increased solar activity in 2014–15. This spot produced enough counts that it could cause mis-centering during all phases of the FUV LP3 (& LP4) spectroscopic TAs. This mis-centerings could be in significant in either the AD or XD. All affected LP3 FUVB TA subarrays were adjusted on April 20, 2015 (2015.110)[31].

In FUVB detector coordinates, the approximate location of the hot-spot is at [X,Y]=[14895,482]. As this is near the detector edge, we are able to avoid this hotspot by stopping the last subarray

[31] See *PR#*80571 for futher details.

Table 14. FUV WCA Subarrays for LP1–4.

| | A1 Subarray | | | | B1 Subarray | | | |
|---|---|---|---|---|---|---|---|---|
| *OPT_ELEM* | XC | YC | XS | YS | XC | YC | XS | YS |
| (1) | (2) | (3) | (4) | (5) | (6) | (7) | (8) | (9) |
| | | | | LP1 | | | | |
| G130M | 1201 | 541[a] | 13799 | 44 | 1501 | 585 | 13799 | 44 |
| G160M | 1201 | 535[a] | 13799 | 44 | 1501 | 579[a] | 13799 | 44 |
| G140L | 1201 | 547[a] | 13799 | 44 | ... | ... | ... | ... |
| G140L | 4701 | 547[b] | 10299[b] | 44 | ... | ... | ... | ... |
| | | | | LP2[c] | | | | |
| G130M | 1201 | 581 | 13799 | 44 | 1501 | 630 | 13799 | 44 |
| G160M | 1201 | 568 | 13799 | 44 | 1501 | 617 | 13799 | 44 |
| G140L | 4701 | 587 | 10299 | 44 | ... | ... | ... | ... |
| | | | | LP3[d] | | | | |
| G130M | 1201 | 515 | 13799 | 44 | 1501 | 567 | 13799 | 44 |
| G160M | 1201 | 504 | 13799 | 44 | 1501 | 559 | 13799 | 44 |
| G140L | 4701 | 521 | 10299 | 44 | ... | ... | ... | ... |
| | | | | LP4[e] | | | | |
| G130M | 1201 | 483 | 13799 | 52 | 1501 | 539 | 13799 | 52 |
| G160M | 1201 | 475 | 13799 | 52 | 1501 | 534 | 13799 | 52 |
| G140L | 4701 | 491 | 10299 | 52 | ... | ... | ... | ... |

[a]These values were updated on 2009.201 (July 20, 2009) with *PR#*63095, some very early COS calibration and ERO datasets used slightly different TA subarrays.

[b]Additional G140L updates were made on Dec. 4, 2012 (2012.339) with *PR#*72193 to futher optimize the G140L subarrays.

[c]Updated for LP2 operations on July 18, 2012 (2012.200) with *PR#*70548.

[d]Updated for LP3 operations on Aug. 26, 2014 (2014.238) with *PR#*78747.

[e]Updated for LP4 operations on Feb. 20, 2017 (2017.051) with *PR#*86945.

Table 15. FUVA PSA/BOA Subarrays for LP1–4

| *OPT_ELEM* | *CENWAVE* | A1 Subarray | | | | A2 Subarray | | | |
|---|---|---|---|---|---|---|---|---|---|
| | (Å) | XC | YC | XS | YS | XC | YC | XS | YS |
| (1) | (2) | (3) | (4) | (5) | (6) | (7) | (8) | (9) | (10) |
| | | | | LP1 | | | | | |
| G130M | 1291 | 1201 | 6555[b] | 437[a] | 76 | 4078 | 8896[b] | 437[a] | 76 |
| G130M | 1300 | 1201 | 7559[b] | 437[a] | 76 | 4078 | 9900[b] | 437[a] | 76 |
| G130M | 1309 | 1201 | 8562[b] | 437[a] | 76 | 4097[b] | 10903[b] | 437[a] | 76 |
| G130M | 1318 | 1201 | 9465[b] | 437[a] | 76 | 3194[b] | 11806[b] | 437[a] | 76 |
| G130M | 1327 | 1201 | 10489[b] | 437[a] | 76 | 2170[b] | 12830[b] | 437[a] | 76 |
| G160M | ALL | 1201 | 13799 | 432[a,b] | 76 | … | … | … | … |
| G140L | 1105 | 1201 | 10458[c] | 445[a,b] | 76 | 457 | 14543 | 445[a,b] | 76 |
| G140L | 1230[g] | 1201 | 12216[c] | 445[a,b] | 76 | … | … | … | … |
| G140L | 1280 | 1201 | 12216[c] | 445[a,b] | 76 | … | … | … | … |
| G140L | 1105 | 4701[c] | 6958[c] | 445[a,b] | 76 | 457 | 14543 | 445[a,b] | 76 |
| G140L | 1230[g] | 4701[c] | 8716[c] | 445[a,b] | 76 | … | … | … | … |
| G140L | 1280 | 6201[c] | 7400[c] | 445[a,b] | 76 | … | … | … | … |
| | | | | LP2[d] | | | | | |
| G130M | 1291 | 1201 | 472 | 6555 | 76 | 8896 | 472 | 4078 | 76 |
| G130M | 1300 | 1201 | 472 | 7559 | 76 | 9900 | 472 | 4078 | 76 |
| G130M | 1309 | 1201 | 472 | 8562 | 76 | 10903 | 472 | 4097 | 76 |
| G130M | 1318 | 1201 | 472 | 9465 | 76 | 11806 | 472 | 3194 | 76 |
| G130M | 1327 | 1201 | 472 | 10489 | 76 | 12830 | 472 | 2170 | 76 |
| G160M | ALL | 1201 | 466 | 13799 | 76 | … | … | … | … |
| G140L | 1105 | 4701 | 479 | 6958 | 76 | 14543 | 479 | 457 | 76 |
| G140L | 1280 | 6201 | 479 | 7400 | 76 | … | 34 | … | … |
| G140L | 1105 | 4701 | 479 | 6958 | 76 | 14543 | 479 | 457 | 76 |
| G140L | 1280 | 6201 | 479 | 7400 | 76 | … | … | … | … |
| | | | | LP3[e] | | | | | |
| G130M | 1291 | 1201 | 409 | 6555 | 76 | 8896 | 409 | 4078 | 76 |
| G130M | 1300 | 1201 | 409 | 7559 | 76 | 9900 | 409 | 4078 | 76 |
| G130M | 1309 | 1201 | 409 | 8562 | 76 | 10903 | 409 | 4097 | 76 |
| G130M | 1318 | 1201 | 409 | 9465 | 76 | 11806 | 409 | 3194 | 76 |
| G130M | 1327 | 1201 | 409 | 10489 | 76 | 12830 | 409 | 2170 | 76 |
| G160M | ALL | 1201 | 403 | 13799 | 76 | … | … | … | … |
| G140L | 1105 | 4701 | 418 | 6958 | 76 | 14543 | 418 | 457 | 76 |
| G140L | 1280 | 6201 | 418 | 7400 | 76 | … | … | … | … |
| | | | | LP4[f] | | | | | |
| G130M | 1291 | 1201 | 362 | 6555 | 112 | 8896 | 362 | 4078 | 112 |
| G130M | 1300 | 1201 | 362 | 7559 | 112 | 9900 | 362 | 4078 | 112 |
| G130M | 1309 | 1201 | 362 | 8562 | 112 | 10903 | 362 | 4097 | 112 |
| G130M | 1318 | 1201 | 362 | 9465 | 112 | 11806 | 362 | 3194 | 112 |
| G130M | 1327 | 1201 | 362 | 10489 | 112 | 12830 | 362 | 2170 | 112 |
| G160M | ALL | 1201 | 356 | 13799 | 112 | … | … | … | … |
| G140L | 1105 | 4701 | 372 | 6958 | 112 | 14543 | 372 | 457 | 112 |
| G140L | 1280 | 6201 | 372 | 7400 | 112 | … | … | … | … |

[a]Updated on 2009.201 (July 20, 2009) with *PR#*63095, some very early COS calibration and ERO datasets used slightly different TA subarrays.

[b]Updated early in LP1 on Aug 27, 2009 (2009.2239) with *PR#*63378.

[c]Additional G140L updates were made on Dec. 4, 2012 (2012.339) with *PR#*72193 to futher optimize the G140L subarrays.

[d]Updated for LP2 July 18, 2012 (2012.200) with *PR#*70548.

[e]Updated for LP3 operations on Aug. 26, 2014 (2014.238) with *PR#*78747.

[f]Updated for LP4 operations on Feb. 20, 2017 (2017.051) with *PR#*86945.

[g]Starting with C18, the C1230 *CENWAVE* was replaced with C1280 due to first-order light issues. For further details see the C18 COS Instrument Handbook (Dixon et al., 2010) (*PR#*64041 and *PR#*64659.

Table 16. FUVB PSA/BOA Subarrays for LP1–4.

| *OPT_ELEM* | *CENWAVE* | B1 Subarray | | | | B2 Subarray | | | |
|---|---|---|---|---|---|---|---|---|---|
| | (Å) | XC | YC | XS | YS | XC | YC | XS | YS |
| (1) | (2) | (3) | (4) | (5) | (6) | (7) | (8) | (9) | (10) |
| | | | | LP1[c] | | | | | |
| G130M | 1291 | 5036[b] | 76 | 1501 | 483 | 7477[b] | 76 | 7773[b] | 483[a,b] |
| G130M | 1300 | 6039[b] | 76 | 1501 | 483 | 6474[b] | 76 | 8776[b] | 483[a,b] |
| G130M | 1309 | 7023[b] | 76 | 1501 | 483 | 5490[a] | 76 | 9760[a] | 483[a,b] |
| G130M | 1318 | 7977[b] | 76 | 1501 | 483 | 4536[b] | 76 | 10714[b] | 483[a,b] |
| G130M | 1327 | 7629[b] | 76 | 2792[b] | 483 | 3593[b] | 76 | 11657[b] | 483[a,b] |
| G160M | ALL | 13749 | 76 | 1501 | 477[a,b] | … | … | … | … |
| G140L | 1105 | … | … | … | … | … | … | … | … |
| G140L | 1230[g] | … | … | … | … | … | … | … | … |
| G140L | 1280 | … | … | … | … | … | … | … | … |
| | | | | LP2[c] | | | | | |
| G130M | 1291 | 1501 | 522 | 5036 | 76 | 7773 | 522 | 7477 | 76 |
| G130M | 1300 | 1501 | 522 | 6039 | 76 | 8776 | 522 | 6474 | 76 |
| G130M | 1309 | 1501 | 522 | 7023 | 76 | 9760 | 522 | 5490 | 76 |
| G130M | 1318 | 1501 | 522 | 7977 | 76 | 10714 | 522 | 4536 | 76 |
| G130M | 1327 | 2792 | 522 | 7629 | 76 | 11657 | 522 | 3593 | 76 |
| G160M | ALL | 1501 | 515 | 13749 | 76 | … | … | … | … |
| G140L | 1105 | … | … | … | … | … | … | … | … |
| G140L | 1280 | … | … | … | … | … | … | … | … |
| | | | | LP3[d](Pre FUVB “Hot-Spot”) | | | | | |
| G130M | 1291 | 1501 | 460 | 5036 | 76 | 7773 | 460 | 7477 | 76 |
| G130M | 1300 | 1501 | 460 | 6039 | 76 | 8776 | 460 | 6474 | 76 |
| G130M | 1309 | 1501 | 460 | 7023 | 76 | 9760 | 460 | 5490 | 76 |
| G130M | 1318 | 1501 | 460 | 7977 | 76 | 10714 | 460 | 4536 | 76 |
| G130M | 1327 | 2792 | 460 | 7629 | 76 | 11657 | 460 | 3593 | 76 |
| G160M | ALL | 1501 | 453 | 13749 | 76 | … | … | … | … |
| G140L | 1105 | … | … | … | … | … | … | … | … |
| G140L | 1280 | … | … | … | … | … | … | … | … |
| | | | | LP3[e](Post FUVB “Hot-Spot”)[d] | | | | | |
| G130M | 1291 | 1501 | 460 | 5036 | 76 | 7773 | 460 | 7060[e] | 76 |
| G130M | 1300 | 1501 | 460 | 6039 | 76 | 8776 | 460 | 6057[e] | 76 |
| G130M | 1309 | 1501 | 460 | 7023 | 76 | 9760 | 460 | 5073[e] | 76 |
| G130M | 1318 | 1501 | 460 | 7977 | 76 | 10714 | 460 | 4119[e] | 76 |
| G130M | 1327 | 2792 | 460 | 7629 | 76 | 11657 | 460 | 3176[e] | 76 |
| G160M | ALL | 1501 | 453 | 13332 | 76 | … | … | … | … |
| G140L | 1105 | … | … | … | … | … | … | … | … |
| G140L | 1280 | … | … | … | … | … | … | … | … |
| | | | | LP4[f] | | | | | |
| G130M | 1291 | 1501 | 419 | 5036 | 112 | 7773 | 419 | 7060 | 112 |
| G130M | 1300 | 1501 | 419 | 6039 | 112 | 8776 | 419 | 6057 | 112 |
| G130M | 1309 | 1501 | 419 | 7023 | 112 | 9760 | 419 | 5073 | 112 |
| G130M | 1318 | 1501 | 419 | 7977 | 112 | 10714 | 419 | 4119 | 112 |
| G130M | 1327 | 2792 | 419 | 7629 | 112 | 11657 | 419 | 3176 | 112 |
| G160M | ALL | 1501 | 416 | 13332 | 112 | … | … | … | … |
| G140L | 1105 | … | … | … | … | … | … | … | … |
| G140L | 1280 | … | … | … | … | … | … | … | … |

[a]Updated during SMOV (2009.201) with *PR*#63095.

[b]Updated for LP2 operations on July 18, 2012 (2012.200) with *PR*#70548.

[c]Due to gain sag induced 'Y-walk', the use of the FUVB segment for `ACQ/PEAKXD` (`NUM_POS=1`) TAs was deprecated on April 8, 2011 (2011.098) with *PR*#67985. FUVB is still used for `ACQ/SEARCH` and `ACQ/PEAKD` TA exposures.

[d]Updated for LP3 operations on Aug. 26, 2014 (2014.238) with *PR*#78747.

[e]Updated for post “Hot-Spot” LP3 TA operations on April 20, 2015 (2015.110) with *PR*#80571.

[f]Updated for LP4 operations on Feb. 20, 2017 (2017.051) with *PR*#86945. At LP4, both FUVA and FUVB are supported for all `ACQ/PEAKXD` (*NUM_POS*$>$ 1) TA exposures. These subarrays also avoid the FUVB “Hot-Spot”.

[g]Starting with C18, the C1230 *CENWAVE* was replaced with C1280 due to first-order light issues. For further details see the C18 COS Instrument Handbook (Dixon et al., 2010) (*PR*#64041 and *PR*#64659.

of the FUVB subarrays at X=14833. For the COS FUV gratings and the FUVB TA subarrays, the impacts were:

**G140L:** Not affected as no FUVB TA subarrays are used for G140L

**G160M:** One FUVB subarray is used for each *CENWAVE* with XC1=1501, XS1=13749. These were all changed to XS=13332 (no change in Y).

**G130M:** Two *CENWAVE*-specific FUVB subarrays are used to avoid Geocoronal Ly$\alpha$. The X-size (XS) of the second subarray (XS2) will be trimmed to avoid the hotspot (XC1, XS1, XC2 and all the Y definitions do not change).

As of March 2018, no additional hot-spots have appeared on either FUVA or FUVB that required adjustment of the TA subarrays. Due to the possibility of future hot-spots, the number of allow FUV TA subarrays per segment was increased from two to four on Sept 21, 2015 (2015.264) with *PR#*81263.

# 5 NUV Imaging TA verification

## 5.1 Verifying the ACQ/IMAGE WCA-to-SA Offsets.

The verification of the ACQ/IMAGE WCA-to-SA (PSA or BOA) offsets is a multi-stage bootstrap process similar to the one used to measure the initial offsets in the SMOV enabling program (**P**11471, COS FUV Target Acquisition Algorithm Verification).

## 5.2 Baseline Bootstrap of ACQ/IMAGE Modes

Each visit of each cycles monitoring program directly compares two ACQ/IMAGE combinations. We can bootstrap these back to PSA×MIRA to test the co-alignment of all four combinations. We call this the 'baseline' bootstrapping, the results of which are shown in Table **??**. The values shown in this table are almost exclusively taken from the _RAWACQ.FITS FITS headers of the indicated ACQ/IMAGEs. The values in these header keywords have been converted to COS USER coordinates as given by equations **??** & **??**. In these header keyword names, 'Y' refers to XD and 'X' to AD.

The columns of the Table **??** give:

1. *ROOTNAME* gives the IPPPSSOOT of the COS exposure.
2. *PROPOSID* gives the HST program id (PID).
3. gives the SA×MIRROR configuration (*APERTURE*×*OPT_ELEM*) of the ACQ/IMAGE.
4. gives the measured AD median of the WCA (lamp) image. In the ACQ/IMAGE _RAWACQ.FITS FITS headers, as reported in the *LAMPMXCR* keyword. The header keyword name uses the COS USER coordinate of 'X' for AD.
5. gives the measured XD median of the WCA (lamp) image. This is reported in the *LAMPMYCR* keyword, the header keyword name uses the COS USER coordinate of 'Y' for XD.
6. gives the measured AD centroid[32] of the SA (PSA or BOA) target image. This is reported in the *ACQCENTX* keyword ('X' USER coordinate is AD).
7. gives the measured XD centroid of the SA image. This is reported in the *ACQCENTY* keyword ('Y' USER coordinate is XD).
8. gives the calculated AD centroid of the SA in use, as reported in the *ACQPREFX* keyword. Calculated as the WCA measured position plus the AD component of the WCA-to-SA offset from the FSW.
9. gives the calculated XD centroid of the SA in use, as reported in the *ACQPREFY* keyword. Calculated as the WCA measured position plus the XD component of the WCA-to-SA offset from the FSW.
10. gives the SA-to-WCA AD offset used in this ACQ/IMAGE (calculated as *ACQPREFX-ACQCENTX*).
11. gives the SA-to-WCA XD offset used in this ACQ/IMAGE (calculated as *ACQPREFY-ACQCENTY*).
12. gives the AD centering slew performed by the ACQ/IMAGE, as reported in the *ACQSLEWY* keyword.
13. gives the XD centering slew performed by the ACQ/IMAGE, as reported in the *ACQSLEWX* keyword.
14. *DATE-OBS* gives the date of the observation in YEAR-MOnth-DAy format.

Table 17. Basic ACQ/IMAGE Bootstrapping Results

| *PROPOSID* (PID) | *ROOTNAME* | Configuration *APERTURE* ×*OPT_ELEM* | WCA-Measured[a] AD *LAMPMXCR* | XD *LAMPMYCR* | PSA-Measured AD *ACQCENTX* | XD *ACQCENTY* | PSA-Centered AD *ACQPREFX* | XD *ACQPREFY* | SA-to-WCA AD | XD | TA Centering AD *ACQSLEWX* | XD[b] *ACQSLEWY* | *DATE-OBS* |
|---|---|---|---|---|---|---|---|---|---|---|---|---|---|
| (1) | (2) | (3) | (4) | (5) | (6) | (7) | (8) | (9) | (10) | (11) | (12) | (13) | (14) |
| | | | | | | C21 | | | | | | | |
| 13171 | lc6ka2imq | PSA×MIRA | 650 | 508 | 284.0 | 459.7 | 277.3 | 462.7 | 372.7 | 45.3 | -0.070[c] | 0.158[c] | 2013-09-01 |
| 13171 | lc6ka2ioq | PSA×MIRB | 811 | 304 | 436.5 | 258.2 | 436.9 | 259.0 | 374.1 | 45.0 | -0.019 | -0.009 | 2013-09-01 |
| 13526 | lcgq01qdq | BOA×MIRA | 651 | 520 | 283.2 | 472.9 | 282.6 | 474.5 | 368.4 | 45.5 | -0.038 | 0.013 | 2014-11-19 |
| 13526 | lcgq02huq | BOA×MIRB | 811 | 285 | 440.3 | 237.9 | 444.8 | 238.5 | 366.2 | 46.5 | -0.015 | -0.105 | 2014-11-17 |
| | | | | | | C22 | | | | | | | |
| 13616 | lci4a2e3q | PSA×MIRA | 650 | 517 | 282.9 | 471.7 | 277.3 | 471.7 | 372.7 | 45.3 | 0.001[c] | 0.133[c] | 2014-10-27 |
| 13616 | lci4a2e5q | PSA×MIRB | 809 | 305 | 436.1 | 259.7 | 435.0 | 259.0 | 374.0 | 46.0 | 0.016 | 0.027 | 2014-10-27 |
| 13972 | lcri01g7q | BOA×MIRA | 651 | 517 | 287.2 | 471.0 | 282.6 | 471.5 | 368.4 | 45.5 | -0.011 | 0.109 | 2015-10-06 |
| 13972 | lcri02hgq | BOA×MIRB | 810 | 286 | 444.2 | 240.6 | 443.8 | 239.5 | 366.2 | 46.5 | 0.026 | 0.010 | 2015-10-06 |
| | | | | | | C23 | | | | | | | |
| 14035 | lcsla2bhq | PSA×MIRA | 653 | 505 | 284.8 | 458.8 | 280.3 | 459.7 | 372.7 | 45.3 | -0.020[c] | 0.105[c] | 2015-10-02 |
| 14035 | lcsla2bjq | PSA×MIRB | 813 | 293 | 439.3 | 247.9 | 439.0 | 247.0 | 374.0 | 46.0 | 0.022 | 0.007 | 2015-10-02 |
| 14440 | ld3701h1q | BOA×MIRA | 651 | 518 | 287.1 | 471.7 | 282.6 | 472.5 | 368.4 | 45.5 | -0.018 | 0.105 | 2016-10-18 |
| 14440 | ld3702n9q | BOA×MIRB | 811 | 295 | 446.1 | 248.5 | 444.8 | 248.5 | 366.2 | 46.5 | 0.001 | 0.030 | 2016-10-19 |
| | | | | | | C24 | | | | | | | |
| 14857 | ldozpbf5q | PSA×MIRA | 654 | 515 | 266.2 | 467.3 | 281.3 | 469.7 | 372.7 | 45.3 | -0.058[c] | -0.355[c] | 2017-09-10 |
| 14857 | ldozpbfbq | PSA×MIRB | 813 | 289 | 440.0 | 243.8 | 439.0 | 243.0 | 374.0 | 46.0 | 0.020 | 0.023 | 2017-09-10 |
| 14857 | ldozbadpq | BOA×MIRA | 651 | 524 | 287.4 | 477.9 | 282.6 | 478.5 | 368.4 | 45.5 | -0.013 | 0.113 | 2017-09-04 |
| 14857 | ldozbblmq | BOA×MIRB | 811 | 293 | 444.3 | 246.7 | 444.8 | 246.5 | 366.2 | 46.5 | 0.006 | -0.011 | 2017-09-06 |

[a]Non-repeatability of the OSM and aperture mechanisms, along with environmental factors, result in lamp center offsets of up to 4p in AD and to 10 in XD in these exposures.

[b]BOA ACQ/IMAGEs move the aperture in the XD direction to obtain the WCA lamp image. Occasionally, the aperture mechanism misses the desired location by $\pm$ one step of $\sim 0.05''$.

[c]These PSA×MIRA ACQ/IMAGEs were part of the FGS-to-SI programs and do have a proceeding TA. The TA centerings presented here are to be compared to the FGS-to-SI post processing results presented in Table **??**.

Note. — If the table caption is in the *ITALICS*, this value was taken directly from the indicated _RAWACQ.FITS header keyword. In detector coordinates, +AD is -Y, +XD is -X.

Table 18 ACQ/IMAGE WCA-to-SA FSW Target Offsets

| Direction (AD or XD) | DETector Coordinate | USER[a] Coordinate | MIRROR | PSA | BOA |
|---|---|---|---|---|---|
| | | MIRA | | | |
| AD[c] | Y | -X | MIRA | 45.3 | 45.5 |
| XD[d] | X | -Y | MIRA | 372.7 | 368.4 |
| | MIRB **prior** to Oct-20-2014 (2014.283) | | | | |
| AD | Y | -X | MIRB | 45.0 | 45.5 |
| XD | X | -Y | MIRB | 374.1 | 366.3 |
| | MIRB **after**[b] to Oct-20-2014 (2014.283) | | | | |
| AD | Y | -X | MIRB | 46.0 | 46.5 |
| XD | X | -Y | MIRB | 374.0 | 366.2 |

[a] COS DETector and USER coordinates are related by equations **??** & **??**. As a consequence of these definitions, a given combinations AD or XD WCA-to-SA offset in one coordinate system is equal to the SA-to-WCA offset in the other. For example, the AD PSA×MIRA WCA-to-PSA offset is +45.3 in detector coordinates (Y), as is the SA-to-WCA AD offset in USER coordinates (X).

[b] Installed 2014.283 (*PR#*79116, "Update MIRRORB Cal Target Offsets").

[c] XD direction offsets, measured from calibration lamp median to the SA center, stored in the FSW PCTA_XIMCALTARGETOFFSET table.

[d] AD direction offsets, measured from calibration lamp median to the SA center, stored in the FSW PCTA_YIMCALTARGETOFFSET table.

These measurements have certain limitations, such as the $\pm 0.5p$ measurement uncertainity in both directions when measuring the WCA centroid. The WCA lamp exposures of each cycles program can assist in removing these limitations from the bootstrapping. The PSA ACQ/IMAGE visits leave the shutter open when taking these WCA lamp images so that a co-eval target+lamp TT image is acquired. This allows a direct calculation of the WCA-to-PSA offset using any desired centroiding algoritm. The BOA ACQ/IMAGE visits take sequential lamp and BOA target images to measure the WCA-to-BOA offsets, but these are not co-eval, and the aperture has been moved between the exposures, which often causes a $\pm 1$ step offset. Fortunately, this offset can be tracked with the telemetry keywords and accounted for.

The basic steps in the verification process are:

1. Step1: Perform a PSA×MIRA ACQ/IMAGE **with** a separate WCA lamp image, preferably in TT mode.

   (a) If the PSA×MIRA ACQ/IMAGE was taken as part of an FGS-to-SI alignment program, then use this information to estimate the accuracy of the NUV SIAF entry by comparing the slew from the ACQ/IMAGE to the known offset inferred from evaluation of the FGS-to-SI program data (from Colin Cox).

   (b) Measure the [AD,XD] median of the lamp image (as done in LTAIMCAL), and the center of the target (in the same image) using both the LTAIMAGE 9×9 checkbox +

[32] For details of the ACQ/IMAGE target centroiding algorithm, see the COS IHB (Fox et al., 2017 or Penton & Keyes, 2011)

## Table 19. PSA×MIRA Bootstrapping Measurement Adjustments

| *PROPOSID* | *ROOTNAME* | Cycle | WCA-Measured[a] AD *LAMPMXCR* | XD *LAMPMYCR* | PSA-Measured[d] AD | XD | PSA-Centered AD *ACQPREFX* | XD *ACQPREFY* | SA-to-WCA AD | XD | TA Centering AD *ACQSLEWX* | XD[b] *ACQSLEWY* | *DATE-OBS* |
|---|---|---|---|---|---|---|---|---|---|---|---|---|---|
| (1) | (2) | (3) | (4) | (5) | (6) | (7) | (8) | (9) | (10) | (11) | (12) | (13) | (14) |
| PSA×MIRA | | | | | | | | | | | | | |
| 13171 | lc6ka2imq | C21 | 650 | 508 | 284.0 | 459.7 | 277.3 | 462.7 | 372.7 | 45.3 | $-0.070-(0.077)$ | $0.158-(0.070)$ | 2013-09-01 |
| 13616 | lci4a2e3q | C22 | 650 | 517 | 282.9 | 471.7 | 277.3 | 471.7 | 372.7 | 45.3 | $+0.001-(0.118)$ | $0.133+(0.050)$ | 2014-10-27 |
| 14035 | lcsla2bhq | C23 | 653 | 505 | 284.8 | 458.8 | 280.3 | 459.7 | 372.7 | 45.3 | $-0.020-(0.065)$ | $0.105-(0.051)$ | 2015-10-02 |
| 14857 | ldozpbf5q | C24 | 654 | 515 | 266.2 | 467.3 | 281.3 | 469.7 | 372.7 | 45.3 | $-0.058-()$ | $-0.355-()$ | 2017-09-10 |
| PSA×MIRB | | | | | | | | | | | | | |
| 13171 | lc6ka2ioq | C21 | 811 | 304 | 436.5 | 258.2 | 436.9 | 259.0 | 374.1 | 45.0 | -0.019 | -0.009 | 2013-09-01 |
| 13616 | lci4a2e5q | C22 | 809 | 305 | 436.1 | 259.7 | 435.0 | 259.0 | 374.0 | 46.0 | 0.016 | 0.027 | 2014-10-27 |
| 14035 | lcsla2bjq | C23 | 813 | 293 | 439.3 | 247.9 | 439.0 | 247.0 | 374.0 | 46.0 | 0.022 | 0.007 | 2015-10-02 |
| 14857 | ldozpbfbq | C24 | 813 | 289 | 440.0 | 243.8 | 439.0 | 243.0 | 374.0 | 46.0 | 0.020 | 0.023 | 2017-09-10 |
| BOA×MIRA | | | | | | | | | | | | | |
| 13526 | lcgq01qdq | C21 | 651 | 520 | 283.2 | 472.9 | 282.6 | 474.5 | 368.4 | 45.5 | -0.038 | 0.013 | 2014-11-19 |
| 13972 | lcri01g7q | C22 | 651 | 517 | 287.2 | 471.0 | 282.6 | 471.5 | 368.4 | 45.5 | -0.011 | 0.109 | 2015-10-06 |
| 14440 | ld3701h1q | C23 | 651 | 518 | 287.1 | 471.7 | 282.6 | 472.5 | 368.4 | 45.5 | -0.018 | 0.105 | 2016-10-18 |
| 14857 | ldozbadpq | C24 | 651 | 524 | 287.4 | 477.9 | 282.6 | 478.5 | 368.4 | 45.5 | -0.013 | 0.113 | 2017-09-04 |
| BOA×MIRB | | | | | | | | | | | | | |
| 13526 | lcgq02huq | C21 | 811 | 285 | 440.3 | 237.9 | 444.8 | 238.5 | 366.2 | 46.5 | -0.015 | -0.105 | 2014-11-17 |
| 13972 | lcri02hgq | C22 | 810 | 286 | 444.2 | 240.6 | 443.8 | 239.5 | 366.2 | 46.5 | 0.026 | 0.010 | 2015-10-06 |
| 14440 | ld3702n9q | C23 | 811 | 295 | 446.1 | 248.5 | 444.8 | 248.5 | 366.2 | 46.5 | 0.001 | 0.030 | 2016-10-19 |
| 14857 | ldozbblmq | C24 | 811 | 293 | 444.3 | 246.7 | 444.8 | 246.5 | 366.2 | 46.5 | 0.006 | -0.011 | 2017-09-06 |

[a]Non-repeatability of the OSM and aperture mechanisms, along with environmental factors, result in lamp center offsets of up to 4p in AD and to 10 in XD in these exposures.

[b]BOA `ACQ/IMAGE`s move the aperture in the XD direction to obtain the WCA lamp image. Occasionally, the aperture mechanism misses the desired location by $\pm$ one step of $\sim 0.05''$.

[c]These PSA×MIRA `ACQ/IMAGE`s were part of the FGS-to-SI programs and do **NOT** have a proceeding TA. The TA centering adjustments presented here are to be compared to the FGS-to-SI post processing results presented in Table **??**.

Note. — If the table caption is in the `Courier` font, this value was taken directly from the indicated _RAWACQ.FITS header keyword. In detector coordinates, +AD is -Y, +XD is -X.

## Table 20. COS TA Monitor `ACQ/IMAGE` Data

| *ROOTNAME* | *EXPTYPE* | *OPT_ELEM* | LAMP | Current | Target ET (s) | Lamp ET (s) | WCA AD | WCA XD | SA AD | SA XD | WtP AD | WtP XD | Lamp counts | Lamp cps | WCA bck | Lamp CPS | Lamp BP | Target BP |
|---|---|---|---|---|---|---|---|---|---|---|---|---|---|---|---|---|---|---|
| (1) | (2) | (3) | (4) | (5) | (6) | (7) | (8) | (9) | (10) | (11) | (12) | (13) | (14) | (15) | (16) | (17) | (18) | (19) |
| lcgq01q7q | EXT/SCI | MIRB | P2 | MED | 16 | 16 | 717 | 214 | 763.1 | 588.9 | 46.1 | 374.9 | 4890.0 | 305.6 | 167 | 305.6 | 4.4 | 26.7 |
| lcgq01q9q | EXT/SCI | MIRA | P2 | MED | 150 | 150 | 479 | 370 | 550.3 | 739.9 | 71.3 | 369.9 | 1718.0 | … | … | … | … | 0.2 |
| lcgq02hoq | WAVECAL | MIRA | P2 | LOW | 7 | … | 529 | 372 | 891.6 | 635.6 | 362.6 | 263.6 | 2827.0 | 403.9 | 97 | 403.9 | 9.9 | 0.3 |
| lcgq02hqq | EXT/SCI | MIRB | P2 | LOW | 181 | … | 713 | 211 | 784.4 | 582.7 | 71.4 | 371.7 | 2383.0 | … | … | … | … | 0.2 |
| lcri01g1q | EXT/SCI | MIRB | P2 | MED | 12 | 12 | 722 | 210 | 767.7 | 584.2 | 45.7 | 374.2 | 3016.0 | 251.3 | 166 | 251.3 | 4.2 | 30.0 |
| lcri01g3q | EXT/SCI | MIRA | P2 | MED | 150 | … | 474 | 370 | 552.0 | 735.7 | 78.0 | 365.7 | 1964.0 | … | … | … | … | 0.2 |
| lcri02hcq | EXT/SCI | MIRB | P2 | LOW | 181 | 181 | 715 | 211 | 782.3 | 578.6 | 67.3 | 367.6 | 2406.0 | … | … | … | … | 0.2 |
| ld3701gvq | EXT/SCI | MIRB | P2 | MED | 16 | 16 | 727 | 210 | 772.8 | 584.3 | 45.8 | 374.3 | 4147.0 | 259.2 | 184 | 259.2 | 4.3 | 19.0 |
| ld3701gxq | EXT/SCI | MIRA | P2 | MED | 150 | 150 | 479 | 371 | 551.2 | 735.8 | 72.2 | 364.8 | 1739.0 | … | … | … | … | 0.2 |
| ld3702n1q | WAVECAL | MIRA | P2 | LOW | 14 | … | 515 | 371 | 886.6 | 659.4 | 371.6 | 288.4 | 5589.0 | 399.2 | 167 | 399.2 | 7.7 | 0.2 |
| ld3702n4q | EXT/SCI | MIRB | P2 | LOW | 183 | 183 | 723 | 213 | 774.9 | 577.6 | 51.9 | 364.6 | 2081.0 | … | … | … | … | 0.2 |
| ldozbadjs | EXT/SCI | MIRB | P2 | MED | 16 | 16 | 724 | 210 | 769.8 | 583.4 | 45.8 | 373.4 | 4005.0 | 250.3 | 138 | 250.3 | 4.4 | 20.2 |
| ldozbadlq | EXT/SCI | MIRA | P2 | MED | 150 | 150 | 472 | 371 | 545.1 | 735.6 | 73.1 | 364.6 | 1462.0 | … | … | … | … | 0.2 |
| ldozbblgq | WAVECAL | MIRA | P2 | LOW | 14 | … | 507 | 372 | 748.6 | 911.9 | 241.6 | 539.9 | 5721.0 | 408.6 | 155 | 408.6 | 8.4 | 0.1 |
| ldozbbliq | EXT/SCI | MIRB | P2 | LOW | 183 | … | 713 | 213 | 776.2 | 578.7 | 63.2 | 365.7 | 2283.0 | … | … | … | … | 0.2 |

Note. — **Note to reviewer: Some of the numbers in this table are odd, I am researching.**

flux-weighted centroid algorithm, and a 2D Gaussian fitting profile.

2. Step 2
3. Step 3
4. Step 4
5. Step 5

These results can be combined to show the measured offsets of PSA+MIRB, BOA+MIRA, and BOA+MIRB when compared to the initial PSA+MIRA `ACQ/IMAGE` of Visit ‘A2’ of **P**14035. These results are shown in Table **??**. Combined offsets from PSA+MIRA are provided in both NUV pixels (p) and in arcseconds ($''$).

Table 21. ACQ/IMAGE WCA-to-SA offsets from PSA+MIRA

| Aperture | MIRROR | AD Offset (″) | XD Offset (″) | AD Offset (p) | XD Offset (p) |
|---|---|---|---|---|---|
| | | | C21 | | |
| | | | C22 | | |
| | | | C23 | | |
| | | | C24 | | |
| PSA | B | 0.021 | -0.049 | 0.298 | 0.893 |
| BOA | A | 0.010 | 0.060 | 0.425 | 2.550 |
| BOA | B | 0.036 | 0.070 | 1.530 | 2.975 |

The results of **P**13972 and **P**14035 show that, for ACQ/IMAGEs :

- PSA+MIRA is aligned with PSA+MIRB to [AD, XD] $\leq$ [0.022, 0.007]″ (14035, Visit ‘A2’)
- PSA+MIRB is aligned with BOA+MIRA to [AD, XD] $\leq$ [0.023, 0.100]″ (13972, Visit ‘01’)
- BOA+MIRA is aligned with BOA+MIRB to [AD, XD] $\leq$ [0.022, 0.024]″ (13972, Visit ‘02’)

Discuss *PR#*81834 : COS ACQ/IMAGE WCA2SCI[X,Y] not calculated properly

## 5.3 WCA Lamp Images (aka, Lamp Family Portrait)

The four panels of Figures **??–??** show a ‘family portrait’ of the available COS PtNe Lamp (P1 or P2) + MIRROR (MIRA or MIRB) combinations possible with ACQ/IMAGE. Panel titles give the lamp and mirror combination, along with the current setting (in milli-amps, mA) and the exposure times. The images and subarrays are in ‘detector’ coordinates, as used on-board COS. The images show the observed counts/pixel/s (cps) as given by the colorbar on the bottom. The red dashed boxes show the given cycles’ ACQ/IMAGE WCA subarrays. At the top of the subarrays, text provides the count rate in the brightest pixel (BP) in units of counts per second per NUV MAMA pixel (cps). The blue histogram on the bottom edge shows the cross-dispersion (XD) lamp profile in detector ‘X’ coordinates, while the green histogram on the left edge shows the along-dispersion (AD) lamp profile in detector ‘Y’ coordinates. The cross-hairs show the median location of the given configurations’ lamp events within the TA subarray. PtNe#2 (P2) lamp was used for all ACQ/IMAGEs during C21-24, and was operated at LOW current (6 mA) for the using MIRA images and LOW current (3 mA) or MEDium current (10 mA) for the MIRB, depending on the Cycle. Note the separate MIRB images in about a 2:1 ratio, and the asymmetric (toward -XD) scattered light.

**Note to reviewers: Placeholder text alert for possible further analysis to be added. Most of it overlaps with the subarray section, so** . . .

Table 22. COS TA `ACQ/IMAGE` Monitoring Results Summary

| `ACQ/` Mode | COS Channel | Optical Configuration | Direction AD or XD | Measured Offset[a] (mas) | Requirement (mas) | Goal (mas) |
|---|---|---|---|---|---|---|
| | | | C21 | | | |
| | | | C22 | | | |
| | | | C23 | | | |
| | | | C24 | | | |
| IMAGE | NUV | PSA+MIRA | AD | 20±14 | 41–105 | 40 |
| IMAGE | NUV | PSA+MIRB | AD | 10±14 | 41–105 | 40 |
| IMAGE | NUV | BOA+MIRA | AD | 20±14 | 41–105 | 40 |
| IMAGE | NUV | BOA+MIRB | AD | 15±14 | 41–105 | 40 |
| IMAGE | NUV | PSA+MIRA | XD | 75±14 | 300 | 100 |
| IMAGE | NUV | PSA+MIRB | XD | 20±14 | 300 | 100 |
| IMAGE | NUV | BOA+MIRA | XD | 95±14 | 300 | 100 |
| IMAGE | NUV | BOA+MIRB | XD | 12±14 | 300 | 100 |
| PEAKXD | NUV | G185M | XD | 70±17 | 300 | 100 |
| PEAKXD | NUV | G225M | XD | 60±17 | 300 | 100 |
| PEAKXD | NUV | G285M | XD | 20±17 | 300 | 100 |
| PEAKXD | NUV | G230L | XD | 20±17 | 300 | 100 |
| PEAKXD | FUVA | G130M | XD | -30±71 | 300 | 100 |
| PEAKXD | FUVA | G160M | XD | -20±71 | 300 | 100 |
| PEAKXD | FUVA | G140L | XD | -170±71 | 300 | 100 |

[a]The quoted error bars are associated with a 0.5 uncertainty when measuring the integer WCA coordinate, and 1/3 of an NUV pixel when using the `ACQ/IMAGE` checkbox centering algorithm. Added in quadrature, the approximate `ACQ/IMAGE` measurement error is $\approx 0.6$ NUV pixels, or 14 (mas). Each `ACQ/PEAKXD` WCA-to-SA measurement contains an error estimate of $\sqrt{2} * 0.5$ times the plate scale of the detector in use (one half pixel or digital-element uncertainty for each measurement of an integer quantity). For the NUV channel, this is 23.5 (mas)/p or $\sqrt{2}*0.5*23.5 = 17$ (mas). For the FUV channel, this is $\approx \sqrt{2} * 0.5 * 100 \approx 71$ (mas).

Table 23. COS TA Monitor `ACQ/IMAGE` Data

| *ROOTNAME* (1) | *EXPTYPE* (2) | *OPT_ELEM* (3) | LAMP (4) | Current (5) | Target ET (s) (6) | Lamp ET (s) (7) | WCA AD (8) | WCA XD (9) | SA AD (10) | SA XD (11) | WtP AD (12) | WtP XD (13) | Lamp counts (14) | Lamp cps (15) | WCA bck (16) | Lamp CPS (17) | Lamp BP (18) | Target BP (19) |
|---|---|---|---|---|---|---|---|---|---|---|---|---|---|---|---|---|---|---|
| lcgq01q7q | EXT/SCI | MIRB | P2 | Med | 16 | 16 | 717 | 214 | 763.1 | 588.9 | 46.1 | 374.9 | 4890.0 | 305.6 | 167 | 305.6 | 4.4 | 26.7 |
| lcgq01q9q | EXT/SCI | MIRA | P2 | Med | 150 | 150 | 479 | 370 | 550.3 | 739.9 | 71.3 | 369.9 | 1718.0 | … | … | … | … | 0.2 |
| lcgq01qbq | WAVECAL | MIRA | P2 | Low | 7 | … | 503 | 372 | 596.4 | 869.2 | 93.4 | 497.2 | 2964.0 | 423.4 | 61 | 423.4 | 7.7 | 0.3 |
| lcgq01qfq | WAVECAL | MIRA | P2 | Low | 7 | … | 503 | 372 | 652.2 | 793.2 | 149.2 | 421.2 | 2882.0 | 411.7 | 71 | 411.7 | 7.9 | 0.3 |
| lcgq01qhq | EXT/SCI | MIRB | P2 | Med | 12 | 12 | 718 | 212 | 762.9 | 589.3 | 44.9 | 377.3 | 3391.0 | 282.6 | 151 | 282.6 | 3.9 | 19.9 |
| lcgq02hoq | WAVECAL | MIRA | P2 | Low | 7 | … | 529 | 372 | 891.6 | 635.6 | 362.6 | 263.6 | 2827.0 | 403.9 | 97 | 403.9 | 9.9 | 0.3 |
| lcgq02hqq | EXT/SCI | MIRB | P2 | Low | 181 | … | 713 | 211 | 784.4 | 582.7 | 71.4 | 371.7 | 2383.0 | … | … | … | … | 0.2 |
| lcgq02hsq | WAVECAL | MIRB | P2 | Med | 12 | … | 738 | 212 | 898.7 | 439.2 | 160.7 | 227.2 | 3683.0 | 306.9 | 165 | 306.9 | 4.8 | 0.2 |
| lcgq02hwq | WAVECAL | MIRB | P2 | Med | 12 | … | 738 | 213 | 927.8 | 656.8 | 189.8 | 443.8 | 3575.0 | 297.9 | 145 | 297.9 | 3.9 | 0.2 |
| lcgq02hyq | WAVECAL | MIRA | P2 | Low | 10 | … | 522 | 372 | 451.2 | 711.3 | -70.8 | 339.3 | 4173.0 | 417.3 | 147 | 417.3 | 7.7 | 0.2 |
| lcgq02icq | WAVECAL | MIRA | P1 | Low | 10 | … | 537 | 374 | 803.3 | 768.3 | 266.3 | 394.3 | 26040.0 | 2604.0 | 120 | 2604.0 | 46.7 | 0.2 |
| lcgq02ieq | WAVECAL | MIRA | P2 | Low | 10 | … | 538 | 374 | 559.7 | 667.1 | 21.7 | 293.1 | 4036.0 | 403.6 | 122 | 403.6 | 7.4 | 0.2 |
| lcgq02igq | WAVECAL | MIRB | P1 | Low | 30 | … | 747 | 215 | 879.3 | 654.8 | 132.3 | 439.8 | 2659.0 | 88.6 | 364 | 88.6 | 1.3 | 0.1 |
| lcgq02iiq | WAVECAL | MIRB | P2 | Med | 20 | … | 747 | 215 | 539.0 | 725.6 | -208.0 | 510.6 | 6620.0 | 331.0 | 250 | 331.0 | 4.5 | 0.1 |
| lcri01g1q | EXT/SCI | MIRB | P2 | Med | 12 | 12 | 722 | 210 | 767.7 | 584.2 | 45.7 | 374.2 | 3016.0 | 251.3 | 166 | 251.3 | 4.2 | 30.0 |
| lcri01g3q | EXT/SCI | MIRA | P2 | Med | 150 | … | 474 | 370 | 552.0 | 735.7 | 78.0 | 365.7 | 1964.0 | … | … | … | … | 0.2 |
| lcri01g5q | WAVECAL | MIRA | P2 | Low | 10 | … | 506 | 372 | 768.5 | 842.0 | 262.5 | 470.0 | 4100.0 | 410.0 | 117 | 410.0 | 9.8 | 0.2 |
| lcri01g9q | WAVECAL | MIRA | P2 | Low | 10 | … | 506 | 371 | 278.3 | 582.7 | -227.7 | 211.7 | 3960.0 | 396.0 | 148 | 396.0 | 9.2 | 0.2 |
| lcri01gcq | EXT/SCI | MIRB | P2 | Med | 14 | 12 | 723 | 212 | 767.4 | 588.9 | 44.4 | 376.9 | 3381.7 | 281.8 | 148 | 281.8 | 4.0 | 28.3 |
| lcri02haq | WAVECAL | MIRA | P2 | Low | 14 | … | 526 | 372 | 644.1 | 719.4 | 118.1 | 347.4 | 5730.0 | 409.3 | 195 | 409.3 | 8.4 | 0.1 |
| lcri02hcq | EXT/SCI | MIRB | P2 | Low | 181 | 181 | 715 | 211 | 782.3 | 578.6 | 67.3 | 367.6 | 2406.0 | … | … | … | … | 0.2 |
| lcri02heq | WAVECAL | MIRB | P2 | Med | 24 | … | 737 | 213 | 853.4 | 647.7 | 116.4 | 434.7 | 7167.0 | 298.6 | 308 | 298.6 | 4.6 | 0.1 |
| lcri02hiq | WAVECAL | MIRB | P2 | Med | 24 | … | 737 | 213 | 606.7 | 645.2 | -130.3 | 432.2 | 7316.0 | 304.8 | 295 | 304.8 | 4.5 | 0.1 |
| lcri02hkq | WAVECAL | MIRA | P2 | Low | 14 | … | 519 | 372 | 551.0 | 580.0 | 32.0 | 208.0 | 5840.0 | 417.1 | 203 | 417.1 | 7.9 | 0.1 |
| lcri02hyq | WAVECAL | MIRA | P1 | Low | 14 | … | 463 | 372 | 683.3 | 807.3 | 220.3 | 435.3 | 36245.0 | 2588.9 | 201 | 2588.9 | 45.5 | 0.1 |
| lcri02i0q | WAVECAL | MIRA | P2 | Low | 24 | … | 463 | 372 | 781.3 | 778.6 | 318.3 | 406.6 | 9864.0 | 411.0 | 303 | 411.0 | 6.9 | 0.1 |
| lcri02i2q | WAVECAL | MIRB | P1 | Low | 30 | … | 672 | 213 | 486.2 | 739.8 | -185.8 | 526.8 | 2864.0 | 95.5 | 415 | 95.5 | 1.3 | 0.1 |
| lcri02i4q | WAVECAL | MIRB | P2 | Med | 24 | … | 671 | 212 | 884.3 | 415.3 | 213.3 | 203.3 | 8082.0 | 336.8 | 312 | 336.8 | 4.9 | 0.1 |
| ld3701gvq | EXT/SCI | MIRB | P2 | Med | 16 | 16 | 727 | 210 | 772.8 | 584.3 | 45.8 | 374.3 | 4147.0 | 259.2 | 184 | 259.2 | 4.3 | 19.0 |
| ld3701gxq | EXT/SCI | MIRA | P2 | Med | 150 | 150 | 479 | 371 | 551.2 | 735.8 | 72.2 | 364.8 | 1739.0 | … | … | … | … | 0.2 |
| ld3701gzq | WAVECAL | MIRA | P2 | Low | 9 | … | 505 | 372 | 413.8 | 701.7 | -91.2 | 329.7 | 3667.0 | 407.4 | 94 | 407.4 | 8.1 | 0.2 |
| ld3701h3q | WAVECAL | MIRA | P2 | Low | 10 | … | 505 | 372 | 802.6 | 780.0 | 297.6 | 408.0 | 3999.0 | 399.9 | 107 | 399.9 | 7.6 | 0.2 |
| ld3701h5q | EXT/SCI | MIRB | P2 | Med | 16 | 1 6 | 728 | 212 | 773.4 | 589.0 | 45.4 | 377.0 | 4343.0 | 271.4 | 185 | 271.4 | 4.6 | 19.1 |
| ld3702n1q | WAVECAL | MIRA | P2 | Low | 14 | … | 515 | 371 | 886.6 | 659.4 | 371.6 | 288.4 | 5589.0 | 399.2 | 167 | 399.2 | 7.7 | 0.2 |
| ld3702n4q | EXT/SCI | MIRB | P2 | Low | 183 | 183 | 723 | 213 | 774.9 | 577.6 | 51.9 | 364.6 | 2081.0 | … | … | … | … | 0.2 |
| ld3702n7q | WAVECAL | MIRB | P2 | Med | 24 | … | 728 | 212 | 778.9 | 703.3 | 50.9 | 491.3 | 7288.0 | 303.7 | 277 | 303.7 | 4.5 | 0.1 |
| ld3702nbq | WAVECAL | MIRB | P2 | Med | 24 | … | 728 | 212 | 248.1 | 419.3 | -479.9 | 207.3 | 7140.0 | 297.5 | 274 | 297.5 | 4.5 | 0.1 |
| ld3702neq | WAVECAL | MIRA | P2 | Low | 14 | … | 507 | 372 | 911.7 | 878.5 | 404.7 | 506.5 | 5622.0 | 401.6 | 153 | 401.6 | 8.1 | 0.1 |
| ld3702o1q | WAVECAL | MIRA | P1 | Low | 14 | … | 531 | 371 | 485.9 | 883.6 | -45.1 | 512.6 | 37530.0 | 2680.7 | 172 | 2680.7 | 45.6 | 0.1 |
| ld3702o3q | WAVECAL | MIRA | P2 | Low | 24 | … | 531 | 371 | 665.9 | 888.6 | 134.9 | 517.6 | 9841.0 | 410.0 | 273 | 410.0 | 6.9 | 0.1 |
| ld3702o5q | WAVECAL | MIRB | P1 | Low | 30 | … | 744 | 211 | 651.6 | 609.1 | -92.4 | 398.1 | 2375.0 | 79.2 | 319 | 79.2 | 1.5 | 0.1 |
| ld3702o7q | WAVECAL | MIRB | P2 | Med | 24 | … | 743 | 211 | 940.2 | 700.2 | 197.2 | 489.2 | 6674.0 | 278.1 | 283 | 278.1 | 4.2 | 0.1 |
| ldozbadjs | EXT/SCI | MIRB | P2 | Med | 16 | 16 | 724 | 210 | 769.8 | 583.4 | 45.8 | 373.4 | 4005.0 | 250.3 | 138 | 250.3 | 4.4 | 20.2 |
| ldozbadlq | EXT/SCI | MIRA | P2 | Med | 150 | 150 | 472 | 371 | 545.1 | 735.6 | 73.1 | 364.6 | 1462.0 | … | … | … | … | 0.2 |
| ldozbadnq | WAVECAL | MIRA | P2 | Low | 9 | … | 499 | 372 | 889.8 | 583.2 | 390.8 | 211.2 | 3688.0 | 409.8 | 76 | 409.8 | 7.7 | 0.2 |
| ldozbadrq | WAVECAL | MIRA | P2 | Low | 10 | … | 498 | 372 | 311.8 | 608.8 | -186.2 | 236.8 | 4009.0 | 400.9 | 97 | 400.9 | 7.0 | 0.2 |
| ldozbadtq | EXT/SCI | MIRB | P2 | Med | 16 | 16 | 725 | 212 | 769.8 | 588.9 | 44.8 | 376.9 | 4367.0 | 272.9 | 121 | 272.9 | 3.7 | 21.0 |
| ldozbblgq | WAVECAL | MIRA | P2 | Low | 14 | … | 507 | 372 | 748.6 | 911.9 | 241.6 | 539.9 | 5721.0 | 408.6 | 155 | 408.6 | 8.4 | 0.1 |
| ldozbbliq | EXT/SCI | MIRB | P2 | Low | 183 | … | 713 | 213 | 776.2 | 578.7 | 63.2 | 365.7 | 2283.0 | … | … | … | … | 0.2 |
| ldozbblkq | WAVECAL | MIRB | P2 | Med | 24 | … | 730 | 212 | 585.6 | 716.8 | -144.4 | 504.8 | 6957.0 | 289.9 | 331 | 289.9 | 4.7 | 0.1 |
| ldozbbloq | WAVECAL | MIRB | P2 | Med | 24 | … | 730 | 212 | 703.1 | 689.2 | -26.9 | 477.2 | 6983.0 | 291.0 | 305 | 291.0 | 4.0 | 0.1 |
| ldozbblqq | WAVECAL | MIRA | P2 | Low | 14 | … | 510 | 372 | 380.6 | 845.9 | -129.4 | 473.9 | 5566.0 | 397.6 | 177 | 397.6 | 7.9 | 0.1 |
| ldozbbm4q | WAVECAL | MIRA | P1 | Low | 16 | … | 503 | 371 | 815.0 | 659.6 | 312.0 | 288.6 | 42548.0 | 2659.2 | 189 | 2659.2 | 44.2 | 0.1 |
| ldozbbm6q | WAVECAL | MIRA | P2 | Low | 26 | … | 503 | 371 | 772.1 | 616.6 | 269.1 | 245.6 | 10476.0 | 402.9 | 300 | 402.9 | 7.6 | 0.1 |
| ldozbbm8q | WAVECAL | MIRB | P1 | Low | 32 | … | 715 | 211 | 252.8 | 463.5 | -462.2 | 252.5 | 2714.0 | 84.8 | 407 | 84.8 | 1.4 | 0.1 |
| ldozbbmaq | WAVECAL | MIRB | P2 | Med | 26 | … | 715 | 211 | 560.5 | 575.1 | -154.5 | 364.1 | 7768.0 | 298.8 | 340 | 298.8 | 3.7 | 0.1 |
| ldozpbf7q | EXT/SCI | MIRA | P2 | Low | 20 | 20 | 511 | 370 | 555.5 | 741.6 | 44.5 | 371.6 | 7790.0 | 389.5 | 269 | 389.5 | 7.3 | 17.2 |
| ldozpbf9q | EXT/SCI | MIRB | P2 | Med | 220 | 40 | 734 | 210 | 779.2 | 582.8 | 45.2 | 372.8 | 12877.2 | 321.9 | 523 | 321.9 | 3.5 | 0.6 |
| ldozpbfdq | EXT/SCI | MIRB | P2 | Med | 220 | 40 | 734 | 211 | 780.3 | 584.0 | 46.3 | 373.0 | 13043.9 | 326.1 | 505 | 326.1 | 3.5 | 0.8 |
| ldozpbffq | EXT/SCI | MIRA | P2 | Low | 20 | 20 | 514 | 370 | 559.3 | 743.2 | 45.3 | 373.2 | 7798.0 | 389.9 | 285 | 389.9 | 7.1 | 23.4 |

Note. — **Note to reviewer: Some of the numbers in this table are odd, I am researching.**

Table 24. Basic ACQ/IMAGE Bootstrapping Results

| *PROPOSID* (PID) (1) | *ROOT NAME* (2) | Configuration[a] #1 (3) | *ACQSLEW* [*X*,*Y*] ($''$) (4) | *APER YPOS* (5) | PID (6) | *ROOT NAME* (7) | Config[a] #2 (8) | *ACQSLEW* [*X*,*Y*] ($''$) (9) | APER *YPOS* (10) | PID (11) | *ROOT NAME* (12) | Config[a] #1 (13) | *ACQSLEW* [*X*,*Y*] ($''$) (14) | APER *YPOS* (15) |
|---|---|---|---|---|---|---|---|---|---|---|---|---|---|---|
| | | | | | | | C21 | | | | | | | |
| **P**13616 | lci4a2e3q | PSA×MIRA | [ 0.001, 0.133] | 127.1 | **P**13616 | lci4a2e5q | PSA×MIRB | [ 0.016, 0.027] | 127.1 | ... | ... | ... | ... | ... |
| **P**13526 | lcgq01q5q | PSA×MIRB | [-0.888, 0.298] | 127.1 | **P**13526 | lcgq01qdq | BOA×MIRA | [-0.038, 0.013] | 126.1 | **P**13526 | lcgq01qjq | PSA×MIRB | [0.027,-0.078] | 126.1 |
| **P**13526 | lcgq02hmq | BOA×MIRA | [ 0.058, 0.305] | 127.1 | **P**13526 | lcgq02huq | BOA×MIRB | [-0.015,-0.105] | 126.1 | **P**13526 | lcgq02i0q | BOA×MIRA | [0.006, 0.063] | 126.1 |
| | | | | | | | C22 | | | | | | | |
| **P**14035 | lcsla2bhq | PSA×MIRA | [-0.020, 0.105] | 125.1 | **P**14035 | lcsla2bjq | PSA×MIRB | [ 0.022, 0.007] | 125.1 | ... | ... | ... | ... | ... |
| **P**13972 | lcri01fzq | PSA×MIRB | [ 0.189,-0.273] | 125.1 | **P**13972 | lcri01g7q | BOA×MIRA | [-0.011, 0.109] | 126.1 | **P**13972 | lcri01geq | PSA×MIRB | [ 0.036,-0.092] | 126.1 |
| **P**13972 | lcri02h8q | BOA×MIRA | [ 0.201,-0.315] | 125.1 | **P**13972 | lcri02hgq | BOA×MIRB | [ 0.026, 0.010] | 126.1 | **P**13972 | lcri02hmq | BOA×MIRA | [-0.018, 0.038] | 126.1 |
| | | | | | | | C23 | | | | | | | |
| **P**14452 | ld3la2ojq | PSA×MIRA | [-0.017, 0.075] | 125.1 | **P**14452 | ld3la2onq | PSA×MIRB | [-0.002, 0.021] | 125.1 | ... | ... | ... | ... | ... |
| **P**14440 | ld3701gtq | PSA×MIRB | [-0.104, 0.088] | 125.1 | **P**14440 | ld3701h1q | BOA×MIRA | [-0.018, 0.105] | 126.1 | **P**14440 | ld3701h7q | PSA×MIRB | [ 0.016,-0.071] | 126.1 |
| **P**14440 | ld3702mzq | BOA×MIRA | [ 0.390, 0.322] | 125.1 | **P**14440 | ld3702n9q | BOA×MIRB | [ 0.001, 0.030] | 126.1 | **P**14440 | ld3702nhq | BOA×MIRA | [-0.012, 0.057] | 126.1 |
| | | | | | | | C24 | | | | | | | |
| **P**14857 | ldozpbf5q | PSA×MIRA | [-0.058,-0.355] | 125.1 | **P**14857 | ldozpbfbq | PSA×MIRB | [ 0.020, 0.023] | 125.1 | **P**14857 | ldozpbfhq | PSA×MIRA | [-0.020,-0.011] | 125.1 |
| **P**14857 | ldozbadhq | PSA×MIRB | [-0.366,-0.967] | 125.1 | **P**14857 | ldozbadpq | BOA×MIRA | [-0.013, 0.113] | 126.1 | **P**14857 | ldozbadvq | PSA×MIRB | [ 0.029,-0.059] | 126.1 |
| **P**14857 | ldozbbleq | BOA×MIRA | [ 0.290, 0.114] | 125.1 | **P**14857 | ldozbblmq | BOA×MIRB | [ 0.006,-0.011] | 126.1 | **P**14857 | ldozbblsq | BOA×MIRA | [-0.015, 0.060] | 126.1 |

[a] Each row test the co-alignment of two ACQ/IMAGE configurations. The first "Configuration#1" exposure centers the target, then the "Configuration#2" exposure measures the co-alignment. A second Configuration#1 ACQ/IMAGE provides a second co-alignment measurement of the BOA configuration #2s.

Note. — The FGS-to-SI alignment programs (**P**13616, **P**14035, & **P**14452) contain a singe pair of ACQ/IMAGEs, while the COS TA monitoring programs contain a third Configuration#1 ACQ/IMAGE.

## 5.4 SIAF Verification

Reference (Mallo 2008).

Table 25. Active COS SIAF[a] Entries

| SIAF APERNAME | YEAR.DAY Activated | V2 (″) | V3 (″) |
|---|---|---|---|
| | NUV LP1 | | |
| LNMAC | 2014.055 | +232.7230 | -237.5150 |
| LNBOA | 2014.055 | +232.7230 | -237.5150 |
| LNPSA | 2014.055 | +232.7230 | -237.5150 |
| LAPTNBOAOF | 2014.055 | +223.3488 | -246.8892 |
| LAPTNPSAOF | 2014.055 | +242.0972 | -228.1408 |
| | FUV LP1 | | |
| LFMAC | 2014.055 | +232.7230 | -237.5150 |
| LFBOA1 | 2016.151 | +232.7230 | -237.5150 |
| LFPSA1 | 2016.151 | +232.7230 | -237.5150 |
| LAPTFBOAF1 | 2016.151 | +223.3488 | -246.8892 |
| LAPTFPSAF1 | 2016.151 | +242.0972 | -228.1408 |
| | FUV LP2 | | |
| LFBOA2 | 2016.151 | +235.1580 | -235.0100 |
| LFPSA2 | 2016.151 | +235.1580 | -235.0100 |
| LAPTFBOAF2 | 2016.151 | +225.7838 | -244.3842 |
| LAPTFPSAF2 | 2016.151 | +244.5322 | -225.6358 |
| | FUV LP3 | | |
| LFBOA3 | 2016.151 | +230.9137 | -239.2749 |
| LFPSA3 | 2016.151 | +230.9137 | -239.2749 |
| LAPTFBOAF3 | 2016.151 | +221.5395 | -248.6491 |
| LAPTFPSAF3 | 2016.151 | +240.2879 | -229.9007 |
| | FUV LP4 | | |
| LFBOA4 | 2017.031 | +229.1328 | -241.0575 |
| LFPSA4 | 2017.031 | +229.1328 | -241.0575 |
| LAPTFBOAF4 | 2017.031 | +219.7586 | -250.4317 |
| LAPTFPSAF4 | 2017.031 | +238.5070 | -231.6833 |

[a]SIAF = Science Instrument Aperture File.

Note. — COS SIAF "Aperture Names" (APERNAME) start with the "L"", and are followed by either an "N" (NUV), "F" (FUV), or "APT"' indicating that the aperture is only used in APT and not for observations. "APT" in the APT entries are immediately followed by an "N" or "F". The SA (BOA or PSA) or MAC then follows. MAC represents the APT MACro aperture used for bright object checking. Finally, FUV entries end in a number giving the LP#, while the NUV "offset" aperturens end with "OF".

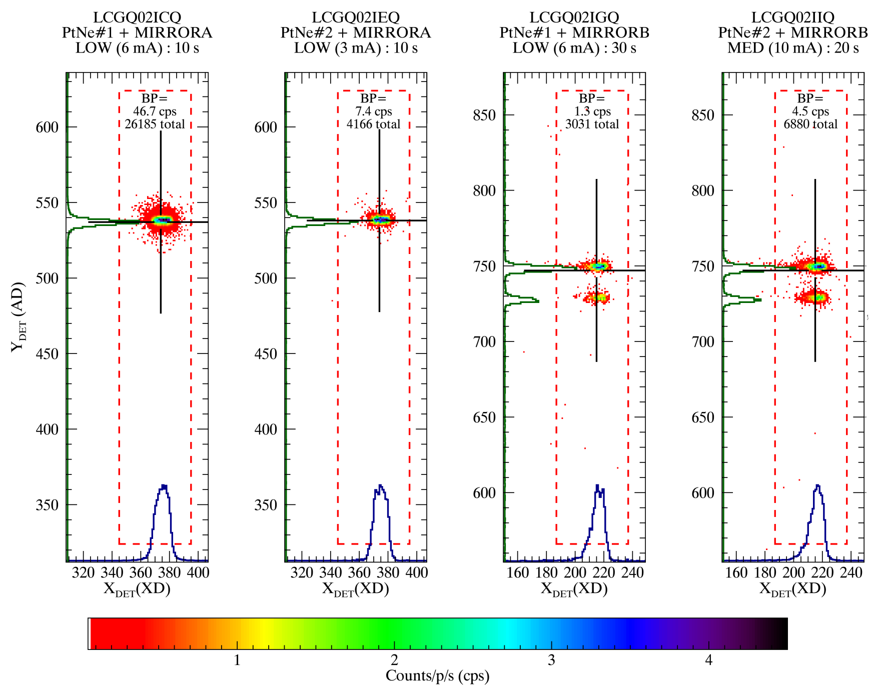


Figure 1 Cycle 21 (**P**13526 PtNe Lamp 'Family Portrait' Counts per second per pixel (cps) NUV images of the internal PtNe lamps (P1 & P2) through the WCA using either MIRRORA (MIRA, left 2 panels) or MIRRORB (MIRB, right 2 panels). The titles give the exposure *ROOTNAME*, configuration, exposure time and lamp current. Cross hairs show median locations and dashed lines show the `LTAIMCAL` TA subarrays. The insert text gives the Brightest Pixel (BP) in cps and the total counts in the subarray. AD and XD profiles are given along each axis, and the color bar at the bottom applies to all four images. Note the separate MIRB images in about a 2:1 ratio, and the asymmetric (toward -XD) scattered light. All panels are in detector (DET) coordinates.

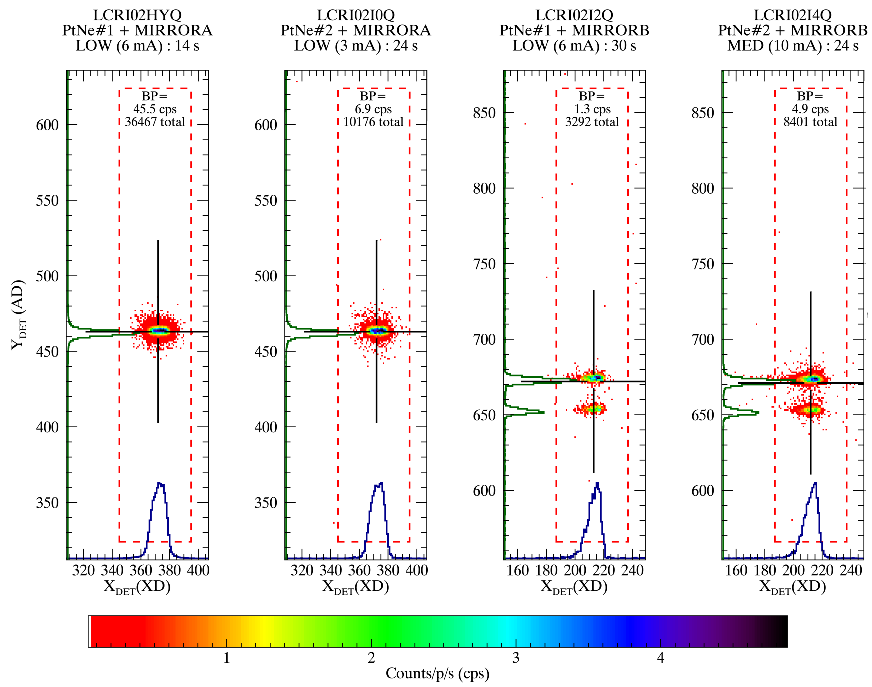


Figure 2 Cycle 22 PtNe Lamp 'Family Portrait' (see Fig **??**).

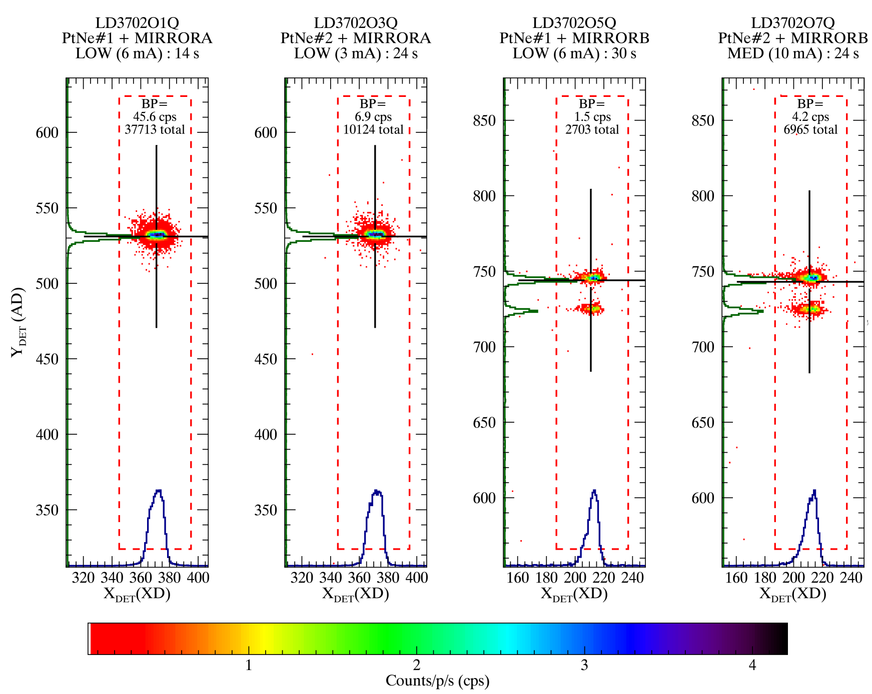


Figure 3 Cycle 23 PtNe Lamp 'Family Portrait' (see Fig **??**).

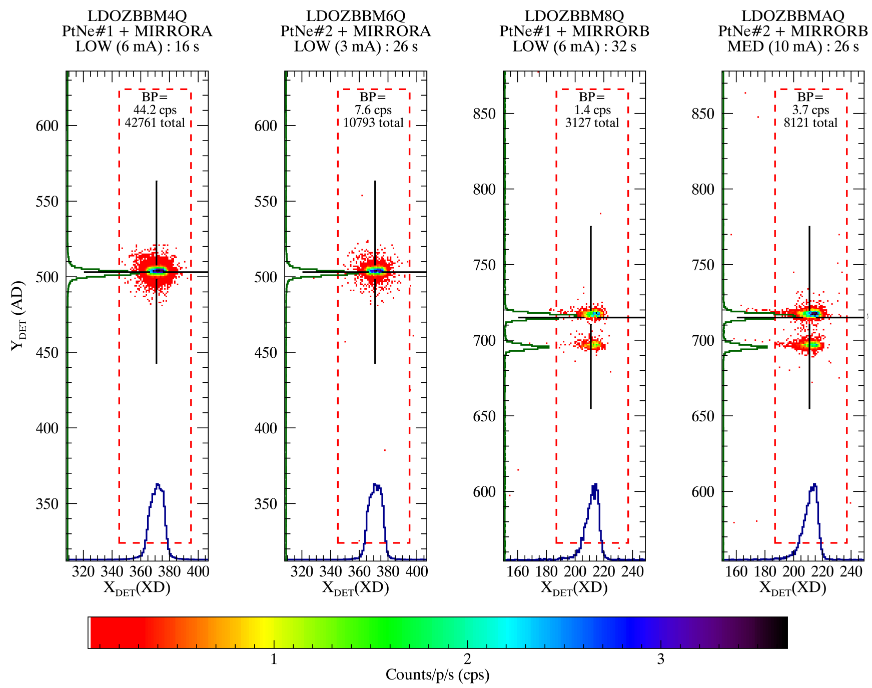


Figure 4 Cycle 24 PtNe Lamp ‘Family Portrait’ (see Fig **??**).

Table 26. FGS-to-SI Program Initial Pointing Determinations

| PID | YEAR.DAY | DATE-OBS | Initial Pointing V2 (″) | Initial Pointing V3 (″) | Miss-Distance V2 (″) | Miss-Distance V3 (″) | Miss-Distance AD (″) | Miss-Distance XD(″) | SIAF Dates[a] | Active SIAF Entry V2 (″) | Active SIAF Entry V3 (″) |
|---|---|---|---|---|---|---|---|---|---|---|---|
| (1) | (2) | (3) | (4) | (5) | (6) | (7) | (8) | (9) | (10) | (11) | (12) |
| **P**11878 | 2009.338 | 04-Dec-2009 | 232.581 | -237.544 | -0.191 | -0.033 | -0.158 | -0.112 | 3-Aug-2009 | 232.772 | -237.511 |
| **P**11878 | 2010.074 | 15-Mar-2010 | 232.488 | -237.462 | -0.284 | 0.049 | -0.166 | -0.235 | ... | 232.772 | -237.511 |
| **P**11878 | 2010.110 | 20-Apr-2010 | 232.481 | -237.457 | -0.291 | 0.054 | -0.168 | -0.244 | ... | 232.772 | -237.511 |
| **P**11878 | 2010.309 | 05-Nov-2010 | 232.604 | -237.561 | -0.168 | -0.050 | -0.154 | -0.083 | ... | 232.772 | -237.511 |
| **P**12399 | 2011.070 | 11-Mar-2011 | 232.645 | -237.438 | -0.127 | 0.073 | -0.038 | -0.141 | 20-Jun-2011 | 232.772 | -237.511 |
| **P**12399 | 2011.255 | 12-Sep-2011 | 232.737 | -237.507 | 0.091 | -0.062 | 0.021 | 0.108 | 21-Jun-2011 | 232.646 | -237.445 |
| **P**12781 | 2012.087 | 27-Mar-2012 | 232.622 | -237.515 | -0.024 | -0.070 | -0.066 | 0.033 | ... | 232.646 | -237.445 |
| **P**12781 | 2012.268 | 24-Sep-2012 | 232.713 | -237.578 | 0.067 | -0.133 | -0.047 | 0.141 | ... | 232.646 | -237.445 |
| **P**13171 | 2013.061 | 02-Mar-2013 | 232.647 | -237.590 | 0.001 | -0.145 | -0.102 | 0.103 | ... | 232.646 | -237.445 |
| **P**13171 | 2013.244 | 01-Sep-2013 | 232.723 | -237.515 | **0.077**[b] | **-0.070**[b] | 0.005 | 0.104 | 23-Feb-2014 | 232.646 | -237.445 |
| **P**13616 | 2014.055 | 06-Apr-2014 | 232.535 | -237.497 | -0.188 | 0.018 | -0.120 | -0.146 | 24-Feb-2014 | 232.723 | -237.515 |
| **P**13616 | 2014.300 | 27-Oct-2014 | 232.841 | -237.465 | **0.118** | **0.050** | 0.119 | 0.048 | ... | 232.723 | -237.515 |
| **P**14035 | 2015.104 | 14-May-2015 | 232.617 | -237.464 | -0.106 | 0.051 | -0.039 | -0.111 | ... | 232.723 | -237.515 |
| **P**14035 | 2015.275 | 02-Oct-2015 | 232.788 | -237.462 | **0.065** | **0.053** | 0.083 | 0.008 | ... | 232.723 | -237.515 |
| **P**14452 | 2016.092 | 01-Apr-2016 | 232.742 | -237.485 | 0.019 | 0.030 | 0.035 | -0.008 | ... | 232.723 | -237.515 |

[a]Dates in this column show the dates that the [V2,V3] SIAF entries in the this and the following rows were active.

[b]These exposures, and the offsets measured here, were used to adjust the COS SIAF entries on 2014.055 (STScI PR#76982).

Note. — Items in **bold** are used in the analysis of this ISR.

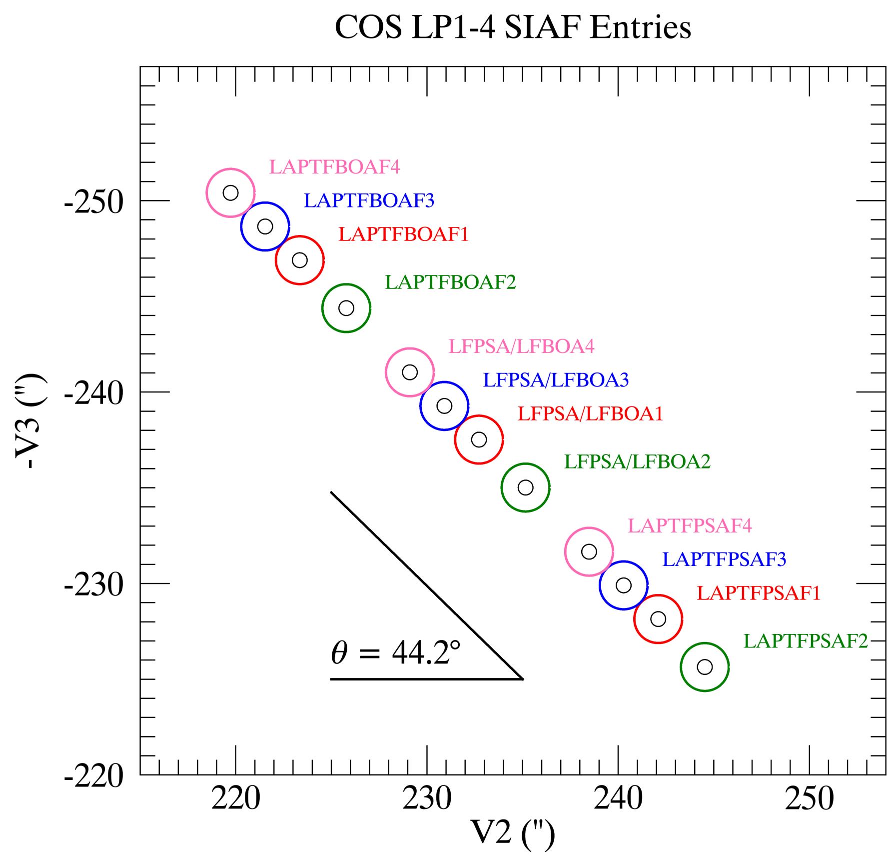


Figure 5 COS SIAF APERTURES . **Note to reviewers, sample SIAF figure1**

Table 27. History of COS SIAF Changes

| YEAR.DAY | STScI *PR#*[a] | Entries Changed | Comment |
|---|---|---|---|
| 2001.001 | N/A | Original 10[b] | Estimates for all COS apertures from Ground Testing |
| 2009.215 | 63138 | Original 10 | On-orbit positions based upon SMOV alignment |
| 2010.055 | 64538 | Original 10 | Update following December 2009 re-alignment |
| 2011.172 | 68498 | Original 10<br>16 New entries[c] | Update original 10 to match June 2011 FGS realignment<br>LP2 prep. Copies of 8 original non-MACro apertures.<br>8 (4 FUV, 4 NUV) have an ’**A**’ (ALTERNATE) added to end.<br>8 (4 FUV, 4 NUV) have a ’**B**’ (BEST) added to end. |
| 2012.086 | 70792 | LF***A** | Initial correction to 4 LP2 FUV LP***A**lternate entries |
| 2012.100 | 70903 | LF***A** | LP2 correction to 4 FUV LP***A**lternate entries. |
| 2012.135 | 71160 | LF***A** | *PR#*70903 adjustment incorrectly applied, corrected. |
| 2012.205 | 71568 | LF***A** and LF***B** | Swap FUV **A** and **B** entries.<br>Afterwards, FUV LP1 entries are in LF***A** and original<br>LP2 entries in LP***B**. |
| 2014.055 | 76982 | All Entries | FGS re-alignment (all apertures) Δ[V2,V3] = [0.077, -0.070]” |
| 2014.188 | 78255 | LF***A** | LP3 initial estimates installed in LF***A** |
| 2014.245 | 78801 | LF***A** | LP3 Final Refinement |
| 2014.265 | 78775 | LF***A** and LF***B** | LP3 Move Best/AlternateSwap<br>After swap, LP1=Original, LP2=LF***A**, & LP3=LF***B**<br>Activated 2014.351 (SIAF entries use 2014.265) |
| 2016.151 | 84188 | Add 32 LP1-8 entries<br>LF***1,2,3** updated<br><br>LF***4,5,6,7,8** | Install new LP# nomeclature<br>Original, **A**lternate, and **B**est entries copied<br>to LP1, LP2, & LP3, respectively<br>LP4-8 entries set to LP3 values |
| 2016.346 | 86315 | LF***4** | Initial LP4 Estimates |
| 2017.058 | 86877 | LF***4** | LP4 Position Final Update (Δ[V2,V3]=[0.0255, -0.0255]) |

[a]The Problem Report #s refer to the SCIOPSDB delivery PRs, not the APT PRs.

[b]The original 10 COS SIAF entries were :

- NUV: LNMAC, LNBOA, LNPSA, LAPTNPSAOF, & LAPTNBOAOF.
- FUV: LFMAC, LFBOA, LFPSA, LAPTFPSAOF, & LAPTFBOAOF.

[c]The 16 new entries were :

- **A**lternate: LNBOA**A**, LNPSA**A**, LFBOA**A**, LFPSA**A**, LAPTFPSAF**A**, LAPTFBOAF**A**, LAPTNPSAF**A**, & LAPTNBOAF**A**.
- **B**est: LNBOA**B**, LNPSA**B**, LFBOA**B**, LFPSA**B**, LAPTFPSAF**B**, LAPTFBOAF**B**, LAPTNPSAF**B**, & LAPTNBOAF**B**.

Note that for the offset apertures, the penultimate letter, “O”, has been removed to create room for the trailing **A** or **B**.

Note. — Trailing characters not part of the original nomenclature are shown in **bold**.

# 6 Spectroscopic TA Verification

After the series of ACQ/IMAGEs that start each visit, the target should be accurately centered. We take advantage of this to monitor certain aspects of COS spectroscopic TAs.

COS spectroscopic TAs consist of up to three stages ACQ/SEARCH, PEAKD, and PEAKXD. The COS spectroscopic ACQ/SEARCH and PEAKD algorithms do not use any FSW patchable constants, and do not flash the internal calibration lamps. The only monitoring required for these TA phases is to ensure that the mechanisms were in their proper positions and that the TA subarrays defined in the HST ground commanding are proper for the mechanism positions used during the acquisitions. As discussed in § **??**, the majority of the details will be addressed for each FUV LP in its enabling ISR, or have already been verified for the NUV and FUV LP1 positions in Penton & Keyes (2011).

COS NUV (LP1) and FUV LP2–4 spectroscopic TA in the XD direction uses ACQ/PEAKXD and requires the use of the XD WCA-to-PSA offsets with the nominal NUM_POS=1 algorithm. These offsets are contained for both the NUV and FUV channels in the FSW patchable constant table PCTA_CALTARGETOFFSET, and are provided for reference for all COS LPs in Table **??**. This ISR only attempts to verify that these offsets were appropriate for all data obtained during the annual monitoring programs.

Each FUV central wavelength setting (*CENWAVE* ) uses a unique OSM1 rotation, whereas all NUV TAs use the same OSM1 rotation independent of *CENWAVE* . However, each NUV *CENWAVE* uses a different OSM2 rotation during TA. Each FUV *CENWAVE* has it's own set of TA subarrays (up to four per segment), while the NUV TA subarrays are not *CENWAVE* specific, but are grating specific.[33]

The verification process is for ACQ/PEAKXD is simple, take a normal spectrum with a target signal-to-noise ratio of least 50 for the entire spectrum (2500 target counts), and directly measure the WCA-to-PSA offset and compare it the FSW value. For NUV exposures, this is almost always STRIPE=B, and for the FUV, only events from FUVA are used at LP2–4. TA subarrays are used to mask out any detector hot-spots or Geocoronal light that could interfere with the centering process. These spectra are also compared to the TA subarrays to verify that they satisfactory.

## 6.1 NUV Spectroscopic TA verification

The P2 WCA lamp and target XD locations for all NUV spectroscopic exposures is given in Table **??**. As shown in the two rightmost "$|\Delta|$" columns of Table **??**, all measured WCA-to-PSA offsets were within 3p in XD there FSW values. This equates to a $< 0.07''$ XD offset due to TA for all NUV monitoring exposures over C21–24.

A visual inspection of the spectra showed all NUV spectra to continue to be well centered in the ACQ/PEAKXD, ACQ/PEAKD, and ACQ/SEARCH NUV spectroscopic subarrays.

**Note to reviewers: Table ?? doesn't actually show the subarray check. This was just a visual check to make sure that the NUV spectrum was well contained in the subarray. If you think that a table comparing the XD line centers to the subarray edges is worthwhile, it can be easily incorporated.**

[33]**Note to reviewer: Do you think it is worthwhile to include the entire PCMECH_OSMTBL in the appendix? If so, i would add a reference to the table and some explanatory text here.**

Table 28. ACQ/PEAKXD WCA-to-PSA offsets

| *OPT_ELEM* | LP1 | LP2 | LP3 |
|---|---|---|---|
| | FUV[f] | | |
| G130M | -898 | -943 | -892 |
| G140L | -884 | -950 | -857 |
| G160M | -898 | -933 | -901 |
| | NUV[n] | | |
| G185M | 3742 | … | … |
| G225M | 3746 | … | … |
| G230L | 3734 | … | … |
| G285M | 3749 | … | … |

[f]Divide the FUV numbers by -10 to get the number of XD rows between the PSA and WCA spectra for a target centered in the aperture.

[n]Divide the NUV numbers by 10 to get the NUV WCA-to-PSA offset.

Note. — The FSW patchable constant PCTA_CALTARGETOFFSETSCALE determines the FSW scaling (currently set to 10). FUV scalings are "negative" due to parity of HST slews relative to the COS coordinate system. **Note to reviewers: Do you think I should keep the numbers in their FSW values (not scaled), or should I go ahead and scale them ?**

## 6.2 FUV Spectroscopic TA verification

The P2 WCA lamp and target XD locations for all centered FUV spectroscopic exposures is given in Table **??**.[34] Explain the last three columns: All FUV monitoring verifications ($|\Delta| = |WtP - eWtp|$) exceeded both the $\pm 0.3''$ requirement, but spectra taken near the end of the LP2 lifetime, and all G140L spectra, exceeded the $\pm 0.1''$ goal.

A visual inspection showed all FUV spectra to continue to be well centered in the FUV spectroscopic subarrays.[35]

[34] The POS_TARG offset spectra are not included in this table as they are beyond the scope of this ISR.

[35] **Note to reviewers: Table ?? doesn't actually show the subarray check. This was just a visual check to make sure that the FUV spectra were well contained in the subarray. If you think that a table comparing the XD line centers to the subarray edges is worthwhile, it can be easily incorporated.**

Table 29. NUV Spectroscopic ACQ/PEAKXD Monitoring

| *ROOTNAME* | *DATE-OBS* | *OPT_ELEM* | LP | WCA[a] (p) | PSA[b] (p) | WtP[c] (p) | eWtP[d] (p) | $\|\Delta\|$[e] (p) | $\|\Delta\|$[f] ($''$)) |
|---|---|---|---|---|---|---|---|---|---|
| (1) | (2) | (3) | (4) | (5) | (6) | (7) | (8) | (9) | (10) |
| | | | | C21 (**P**13526) | | | | | |
| lcgq02i2q | 2014-11-17 | G185M | 1 | 366.0 | 742.0 | 376.0 | 374.20 | 1.80 | 0.04 |
| lcgq02i4q | 2014-11-17 | G225M | 1 | 370.0 | 747.0 | 377.0 | 374.60 | 2.40 | 0.06 |
| lcgq01r6q | 2014-11-19 | G285M | 1 | 355.0 | 728.0 | 373.0 | 374.90 | 1.90 | 0.04 |
| lcgq01qlq | 2014-11-19 | G230L | 1 | 374.0 | 748.0 | 374.0 | 373.40 | 0.60 | 0.01 |
| | | | | C22 (**P**13972) | | | | | |
| lcri02hqq | 2015-10-06 | G185M | 1 | 367.0 | 742.0 | 375.0 | 374.20 | 0.80 | 0.02 |
| lcri02hoq | 2015-10-06 | G225M | 1 | 371.0 | 747.0 | 376.0 | 374.60 | 1.40 | 0.03 |
| lcri01giq | 2015-10-06 | G285M | 1 | 351.0 | 726.0 | 375.0 | 374.90 | 0.10 | <0.01 |
| lcri01ggq | 2015-10-06 | G230L | 1 | 374.0 | 747.0 | 373.0 | 373.40 | 0.40 | 0.01 |
| | | | | C23 (**P**14440) | | | | | |
| ld3702noq | 2016-10-19 | G185M | 1 | 366.0 | 743.0 | 377.0 | 374.20 | 2.80 | 0.07 |
| ld3702nmq | 2016-10-19 | G225M | 1 | 370.0 | 747.0 | 377.0 | 374.60 | 2.40 | 0.06 |
| ld3701hbq | 2016-10-18 | G285M | 1 | 352.0 | 727.0 | 375.0 | 374.90 | 0.10 | <0.01 |
| ld3701h9q | 2016-10-18 | G230L | 1 | 375.0 | 748.0 | 373.0 | 373.40 | 0.40 | 0.01 |
| | | | | C24 (**P**14857) | | | | | |
| ldozbblwq | 2017-09-06 | G185M | 1 | 366.0 | 743.0 | 377.0 | 374.20 | 2.80 | 0.07 |
| ldozbbluq | 2017-09-06 | G225M | 1 | 370.0 | 747.0 | 377.0 | 374.60 | 2.40 | 0.06 |
| ldozbadzq | 2017-09-04 | G285M | 1 | 352.0 | 727.0 | 375.0 | 374.90 | 0.10 | <0.01 |
| ldozbadxq | 2017-09-04 | G230L | 1 | 374.0 | 748.0 | 374.0 | 373.40 | 0.60 | 0.01 |

[a]XD centroid of the WCA spectrum. For NUV spectra, this is the median calibration lamp location.

[b]XD centroid of the target spectrum taken through the PSA, using the same centroid method as the WCA.

[c]WtP is the absolute value of difference in the XD locations of the measured WCA and PSA spectra ($WtP = |PSA - WCA|$)

[d]eWtP = Expected WCA-to-PSA offset from FSW table XIMCALTARGETOFFSET (see Table **??**).

[e]Offset of WtP from a perfectly centered measured in XD rows.

[f]Offset of WtP in arcseconds ($''$). Note that the platescales are different for each grating and LP.

Note. — All spectra were taken at FP-POS=3. All monitoring verifications ($|\Delta| = |WtP - eWtp|$) easily exceeded both the $\pm 0.3''$ requirement and the $\pm 0.1''$ goal.

Table 30. FUV Spectroscopic ACQ/PEAKXD Monitoring

| *ROOTNAME* | *DATE-OBS* | *OPT_ELEM* | LP | WCA[a] (p) | PSA[b] (p) | WtP[c] (p) | eWtP[d] (p) | $\|\Delta\|$[e] (p) | $\|\Delta\|$[f] ($''$) |
|---|---|---|---|---|---|---|---|---|---|
| (1) | (2) | (3) | (4) | (5) | (6) | (7) | (8) | (9) | (10) |
| | | | | C21 (**P**13526) | | | | | |
| lcgq01r8q | 2014-11-19 | G130M | 2 | 602.15 | 508.31 | -93.84 | -92.80 | 1.04 | 0.12 |
| lcgq01raq | 2014-11-19 | G140L | 2 | 608.76 | 513.48 | -95.28 | -93.50 | 1.78 | 0.20 |
| lcgq02i6q | 2014-11-17 | G160M | 2 | 596.07 | 503.35 | -92.71 | -91.80 | 0.91 | 0.11 |
| | | | | C22 (**P**13972) | | | | | |
| lcri01gkq | 2015-10-06 | G130M | 3 | 537.32 | 448.98 | -88.34 | -89.20 | 0.86 | 0.08 |
| lcri01h6q | 2015-10-06 | G140L | 3 | 544.55 | 457.36 | -87.20 | -85.70 | 1.50 | 0.15 |
| lcri02hsq | 2015-10-06 | G160M | 3 | 531.78 | 442.13 | -89.65 | -90.10 | 0.45 | 0.04 |
| | | | | C23 (**P**14440) | | | | | |
| ld3701hdq | 2016-10-18 | G130M | 3 | 536.33 | 447.41 | -88.92 | -89.20 | 0.28 | 0.03 |
| ld3701hfq | 2016-10-18 | G140L | 3 | 543.43 | 455.95 | -87.48 | -85.70 | 1.78 | 0.17 |
| ld3702nqq | 2016-10-19 | G160M | 3 | 531.09 | 440.96 | -90.13 | -90.10 | 0.03 | 0.00 |
| | | | | C24 (**P**14857) | | | | | |
| ldozbae1q | 2017-09-04 | G130M | 3 | 535.26 | 445.66 | -89.61 | -89.20 | 0.41 | 0.04 |
| ldozbae3q | 2017-09-04 | G140L | 3 | 541.76 | 454.25 | -87.51 | -85.70 | 1.81 | 0.18 |
| ldozbblyq | 2017-09-06 | G160M | 3 | 530.84 | 440.75 | -90.09 | -90.10 | 0.01 | 0.00 |

[a]XD centroid of the WCA spectrum.For FUV spectra, this is mean lamp photon location.

[b]XD centroid of the target spectrum taken through the PSA, using the same centroid method as the WCA.

[c]WtP is the absolute value of difference in the XD locations of the measured WCA and PSA spectra ($WtP = |PSA - WCA|$)

[d]eWtP = Expected WCA-to-PSA offset from FSW table XIMCALTARGETOFFSET (see Table **??**).

[e]Offset of WtP from a perfectly centered measured in XD rows.

[f]Offset of WtP in arcseconds ($''$). Note that the platescales are different for each grating and LP.

Note. — All spectra were taken at FP-POS=3. All FUV monitoring verifications ($|\Delta|$ = $|WtP - eWtp|$) exceeded both the $\pm 0.3''$ requirement, but spectra taken near the end of the LP2 lifetime, and all G140L spectra, exceeded the $\pm 0.1''$ goal.

# 7 Results

The main results of the HST Cycles 21–24 COS TA monitoring programs are as follows:

**SIAF: Note to reviewers: Placeholder text pending the insertion of Colins' tweaks.** All COS NUV `ACQ/IMAGE`s use identically-valued SIAF entries (*LFPSA* & *LFBOA*). Where available, the exposures in the FGS-to-SI Alignment programs gave good estimates of the accuracy of the existing NUV LP1 *LFPSA*/*LFBOA* SIAF entries as they performed a PSA×MIRA `ACQ/IMAGE` on a target whose position was already determined by cross-calibration of the other HST Science Instruments (SI). For C21–24, this results of this ISR indicate that the NUV SIAF entry was accurate to at least [AD,XD] = [0.XX,0.YY]″.[36] No SIAF adjustments were identified as being needed for NUV (LP1) or FUV (LP2–3) from the programs of this ISR. However, long term SIAF monitoring is used to track any mechanical drift in the location of the COS aperture mechanism or any changes to the FGS-to-SI alignment that will need adjusting. The last such adjustment was in C22 (February 24, 2014; 2014.055, STScI *PR#*76982), while COS FUV observations were at LP2. At this time, all COS entries (NUV and FUV) were adjusted in [V2,V3] by [0.077, -0.070]".

**Spectroscopic TA Subarrays:** Visual inspection of NUV and FUV images, and a comparison of the NUV and FUV spectra XD centriods, indicate that all spectroscopic TA subarrays were appropriately defined for C21–C24. However, NUV PtNe lamp (WCA) monitoring should be continued, as OSM1 and OSM2 secular drift continues to move the WCA lamp images in AD direction. Combined with the increased detector background of the NUV channel, some of the approved NUV central wavelength settings for COS TA may loss effectiveness, for further details see 2.6 of the C25 COS IHB (Fox et al., 2017). Hot-spot monitoring must be continued for both FUVA and FUVB as COS TA is particularly suseptable to contamination from variable localized detector background.

**NUV Imaging TAs and Subarrays:** The COS `ACQ/IMAGE` tests indicate that the centering achieved with a PSA×MIRB `ACQ/IMAGE` is co-aligned with a PSA×MIRA `ACQ/IMAGE` to within [AD,XD] $\approx$ $[0.010, 0.020]''$, with a measurement error of approximately $0.014''$. `ACQ/IMAGE` tests reveal that BOA×MIRA is co-aligned with PSA×MIRB to within [AD,XD] $\approx$ $[0.015, 0.100]''$, [37] and that BOA×MIRB is co-aligned with BOA×MIRA to within [AD,XD] $\approx$ $[0.007, 0.062]''$. As shown in the PtNe lamp 'family portraits' of Figures **??– ??** are used during the `LTAIMCAL` portion `ACQ/IMAGE` TA FSW routine to locate the position of the aperture mechanism before centering the target. While COS TAs have used the PtNe#2 lamp for all TAs since installation, images of both lamps (P1 and P2) are taken annually with both MIRRORs (MIRA and MIRB) to monitor the observed count rates. No changes of concern were observed in the PtNe lamp count rates between C21–C24. **Note to reviewer: This results may change when Colins SIAF tweaks are included.**

**NUV Spectroscopic TAs:** Spectroscopic TAs for all NUV gratings in all Cycles met both the $0.3''$ requirement and the $0.1''$ goal.

[36] As determined from the initial pointing before the first COS PSA×MIRA `ACQ/IMAGE` of each Cycles program(s).

[37] The larger XD alignment error is due to a frequent 1 aperture XD (XAPER) step mechanism position error (1 step $0.048''$).

**FUV Spectroscopic TAs:** All FUV monitoring verifications ($|\Delta| = |WtP - eWtp|$) exceeded both the $\pm 0.3''$ requirement, but spectra taken near the end of the LP2 lifetime, and all G140L spectra, exceeded the $\pm 0.1''$ goal. [38] Spectroscopic TAs for all FUV gratings met the $0.3''$ requirement and the G130M and G160M gratings achieved the $0.1''$ goal.

# 8 Conclusions.

Through constant monitoring, and periodic FSW, ground commanding, and operations updates, HST+COS TA has performed remarkablely well during Cycles 21–24. The STScI Team thanks the GSFC and STScI personal for there outstanding cooperation and contributions in these efforts

NUV detector background has been the biggest source of concern for NUV TAs, while FUV gain-sag induced Y-walk and inherent detector geometric distortions were the biggest concerns of FUV TAs at LP1–3. At FUV LP4, Y-walk will not be as big a concern as the `NUM_POS=1ACQ/PEAKXD` is not affected by either Y-walk or geometric distortions.

[38] Spectroscopic FUV WCA-to-PSA offsets are determined using a mean photon lamp and/or target XD position in the appropriate subarray. The difference between the positions is compared to the FSW value, accounting for any measured offset in the preceding `ACQ/IMAGE`.

# 9 Acknowledgements

**Notes to reviewers: This section will be completed as the review process continues.** To be acknowledeged: GFSC: Mike Kelly, Ben Teasdel, Olivia Lupie, Scott Swain, STScI: John Bacinski, George Chapman, Merle Reinhart, James White, Sean Lockwood, Brian York, David Sahnow, Karla Peterson, Josh Goldberg.

# 10 Change History for COS ISR 2018-XX

Version 0.01: 30-March-2018 Original Draft Document for Review Version 0.02: 08-April-2018 NUV Image Verification Section partially debuts with tweaks to tables and text (no external comments)

# 11 References

Dixon, W. V., et al. 2010, Cosmic Origins Instrument Handbook (IHB), Version 2.0 (Baltimore, STScI)
Keyes, T., & Penton, S. 2010, COS ISR 2010-14 (v1) (HST+COS Target Acquisition Guidelines, Recommendations, and Interpretation)
Fix, M. B., 2018, COS ISR 2018-03 (v1) (COS NUV Dark Monitor Summary)
Fox, A., et al. 2017, Cosmic Origins Spectosgraph Instrument Handbook (IHB), Version 9.0 (Baltimore, STScI)
Goudfrooij, P., Burgh, E., Aloisi, A., Hartig, G., and Penton, S., 2010, COS 2010-10(v2), "SMOV: COS NUV Imaging Performance" Holland, S. T., et al. 2014, Cosmic Origins Spectrograph Instrument Handbook (IHB), Version 6.0 (Baltimore: STScI)
Lallo, M., 2008, TEL ISR 2008-02,"The COS Pre-flight Aperture Model and SIAF.dat File" Penton, S,, 2001, COS-11-0024A, "TAACOS: Phase I NUV Report"
Penton, S., 2001, COS-11-0014B, "Recommended TA FSW and Operations Changes Based upon the TAACOS Phase I Reports for the FUV and NUV Channels"
Penton, S., 2002, COS-11-0016A, "TAACOS: Phase I FUV Report"
Penton, S., 2010, "The 2010 STScI Calibration Workshop : COS: On-Orbit Performance of Target Acquisitions" Penton, S., & Keyes, T., 2011, COS TIR 2010-03 (On-Orbit Target Acquisitions with HST+COS)
Penton, S., 2016, COS ISR 2016-09 (Cycle 22 HST+COS Target Acquisition Monitoring Summary (**P**13972)
Penton, S., 2017, COS ISR 2017-18 (Cycle 23 HST+COS Target Acquisition Monitoring Summary (**P**14440)
Penton, S., COS ISR 2018-**XX** (HST+COS LP2 Target Acquisition Enabling (LENA3, **P**12797)
Penton, S., COS ISR 2018-**XX** (HST+COS LP3 Target Acquisition Enabling (FENA4, **P**13636)
Penton, S. & White, J. 2018, COS ISR 2018-**XX** (HST+COS LP4 Target Acquisition Enabling (**P**14907
Roman-Duval, J., 2015, COS ISR 2015-02 (Summary of the COS Cycle 20 Calibration Program: **P**13124)
Rose, S., et al., 2017, HST Cycle 25 Phase II Proposal Instructions (V25.0)
Sana, H., et. al., 2015, COS ISR 2015-06 (Summary of the COS Cycle 21 Calibration Program: **P**13526))
Smith, H., et al., 2004, "Hubble Space Telescope Cosmic Origins Spectrograph Contract End Item (CEI) Specification" (NASA STE-63, HST #TM-025984) (2004)
Sonnetrucker, P., et. al., 2016, COS ISR 2016-03 (Summary of the COS Cycle 22 Calibration Program :

**P**13972)
Taylor, J., 2017, COS ISR 2017-13 (v1) (Cycle 23 COS/NUV Spectroscopic Sensitivity Monitor)

Table 31. Cross-Dispersion (XD) Aperture Positions (*APERXPOS*)

| *LIFE_ADJ* | NUV | | FUV | |
|---|---|---|---|---|
| (LP) | PSA[a]/WCA[b] | BOA[c]/FCA[d] | PSA/WCA | BOA/FCA |
| (1) | (2) | (3) | (4) | (5) |
| LP1 | 126 | -153 | 126 | 153 |
| LP2 | 53 | -226 | ... | ... |
| LP3 | 181 | -98 | ... | ... |
| LP4 | 234 | -45 | ... | ... |

[a]PSA=Primary Science Aperture

[b]WCA=Wavelength Calibration Aperture

[c]BOA=Bright Object Aperture

[d]FCA=Flat-field Calibration Aperture

Note. — COS XD aperture positions (*APERXPOS*) are stored in the PCMECH_APMXDISPPOSITION FSW table. Although LP1-8 are defined in that table for both NUV and FUV, only the NUV LP1 and FUV LP1–4 entries listed here have been used for science observations. Values used for FCA calibration observations are different from those listed here, and are commanded via APT special commanding (e.g., during the semi-annual FUV Gain Map programs, **REFERENCE**). Along-Dispersion (AD) values (*APERYPOS*) are stored in the PCMECH_APMDISPPOSITION FSW table. All COS apertures and LPs use *APERYPOS=22*.

# 12 Appendix A : FSW TA Tables